General Disclaimer

One or more of the Following Statements may affect this Document

- This document has been reproduced from the best copy furnished by the organizational source. It is being released in the interest of making available as much information as possible.

- This document may contain data, which exceeds the sheet parameters. It was furnished in this condition by the organizational source and is the best copy available.

- This document may contain tone-on-tone or color graphs, charts and/or pictures, which have been reproduced in black and white.

- This document is paginated as submitted by the original source.

- Portions of this document are not fully legible due to the historical nature of some of the material. However, it is the best reproduction available from the original submission.

NASA CR-137881

HEAT SHIELD CHARACTERIZATION

Outer Planet Atmospheric Entry Probe

By S. A. Mezines, E. L. Rusert and E. F. Disser

Prepared Under Contract No. 2-9027 by

MCDONNELL DOUGLAS ASTRONAUTICS COMPANY – EAST

Saint Louis, Missouri

for

AMES RESEARCH CENTER

NATIONAL AERONAUTICS AND SPACE ADMINISTRATION

N A S A C O N T R A C T O R
R E P O R T

NASA CR-137881
MAY 1976

NASA CR-137881

HEAT SHIELD CHARACTERIZATION

Outer Planet Atmospheric Entry Probe

By S. A. Mezines, E. L. Rusert and E. F. Disser

Prepared by
MCDONNELL DOUGLAS ASTRONAUTICS COMPANY — EAST
St. Louis, Missouri 63166 (314) 232-0232

for Ames Research Center
Moffett Field, California 94035

NATIONAL AERONAUTICS AND SPACE ADMINISTRATION

FOREWORD

This report describes the fabrication of a full scale carbon phenolic heat shield for the Outer Planet Atmospheric Entry Probe. The work (Task 4.2.1) was performed for NASA-ARC under contract NAS 2-9027, as one of twelve Supporting Research and Technology tasks. Technical Monitor of this contract was Dr. John T. Howe, Thermal Protection Branch, NASA-ARC, Moffet Field, California.

The work was performed in the McDonnell Douglas Facilities at St. Louis, Missouri.

TABLE OF CONTENTS

LIST OF FIGURES

LIST OF FIGURES (cont)

LIST OF FIGURES (cont)

SUMMARY

A full scale carbon phenolic heat shield was fabricated for the Outer Planet Probe in order to demonstrate the feasibility of molding large carbon phenolic parts with a new fabrication processing method (multistep). The sphere-cone heat shield was molded as an integral unit with the nose cap plies configured into a double inverse chevron shape to achieve the desired ply orientation. The fabrication activity was successful and the feasibility of the multistep processing technology was established. Delaminations or unbonded plies were visible on the heat shield and resulted from excessive loss of resin and lack of sufficient pressure applied on the part during the curing cycle. These problems will be eliminated by future processing development work based on the experience gained in this program.

A comprehensive heat shield characterization test program was conducted, including: non-destructive tests with the full scale heat shield and thermal and mechanical property tests with small test specimen.

INTRODUCTION AND PROGRAM OBJECTIVES

The NASA's near-term plans include exploration of the Outer Planets - Jupiter, Saturn and Uranus - using entry probes to obtain in situ measurements of the planet's atmosphere. The probes will enter the giant planets at very high speeds and must transverse a very intense heating environment during the brief deceleration period. Survivability of the probe will require a reliable heat protection system of the highest quality. It is essential that such a heat protection system be characterized early in the program to permit an early assessment in order to have sufficient development time to resolve any uncertainties.

McDonnell Douglas Astronautics Company (MDAC) under contract to NASA Ames Research Center (ARC), conducted an initial probe system design study (Reference 1) for the Saturn/Uranus mission requirements. Subsequent probe activities emphasized demonstration of the engineering design concepts through fabrication of actual parts and conductance of proof-of-concept tests. For example, based on the drawings from Reference 1, ARC fabricated and assembled a full scale engineering model (Reference 2) with real structure and simulated equipment boxes having the proper thermal and mass properties. Further validation of the probe system design was accomplished by ARC through the issuance of twelve (12) Supporting Research and Technology tasks, each directed at a critical technological problem area. Task 4.2.1 "Heat Shield Characterization" is one of the twelve tasks and is the subject of this report. The primary objectives of Task 4.2.1 are:

(1) Demonstrate the feasibility of a new and unique fabrication method developed by MDAC by building a full scale carbon phenolic heat shield.
(2) Define the probe heat shield configuration and the environments imposed on the heat shield during each mission phase.
(3) Characterize the heat shield material by test.
(4) Estimate the cost of fabrication and schedule of a flight heat shield based on the fabrication data compiled during this program.

It was mutually agreed between NASA-ARC and MDAC that MDAC should fabricate the Saturn/Uranus heat shield configuration so that it could subsequently be incorporated into the engineering model built by NASA-ARC.

Carbon phenolic was selected as the baseline heat shield material in Reference 1 primarily on the extensive amount of fabrication, predictability and flight experience gained in the DOD Reentry Vehicle Programs. Carbon phenolic is a state-of-the-art material, is competitive in terms of weight and its extensive data base ensures high confidence of achieving success. Subsequent studies to Reference 1 showed that a thicker carbon phenolic heat shield could be used for a Jupiter mission (References 3 and 4); thus, probe commonality was preserved.

The DoD Reentry Vehicle heat shield fabrication experience has been limited to heat shields that have been relatively small in size or simple in shape. In contrast, the probe heat shield is relatively large (89 cm), thick (3 to 6 cm)

and of complex shape (sphere-cone). In the fabrication feasibility studies performed in Reference 1, it was concluded that the probe heat shield represented too large of a mass to be fabricated by the traditional single-step molding technique. Thus, a new fabrication approach was proposed consisting of a series of fifteen compression steps ("multistep") that permits debulking of the prepreg (carbon cloth impregnated with phenolic resin) and assembly of the stack depicted in Figure 1. The entire prepreg stack is cured by application of pressure up to 34 atm, and temperature, up to 177°C, resulting in a homogeneous billet that is machined to the final dimensions. The multistep technique permits compression molding of large parts, conserves material and allows for fabrication of both the nose cap and the conical body as an integral unit with the desired ply orientation. The multistep fabrication concept was progressively demonstrated by first molding small blocks, then building a quarter-scale model of the probe heat shield and finally in the full scale demonstration achieved in this SR&T activity.

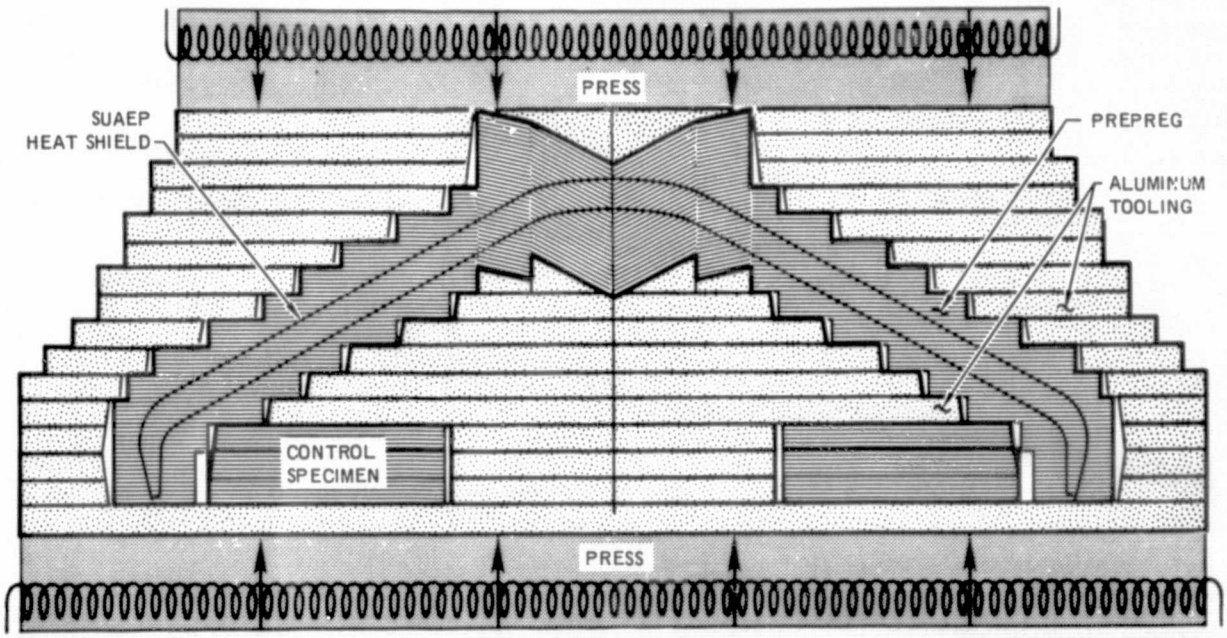

FIGURE 1

MULTISTEP HEAT SHIELD FABRICATION CONCEPT

HEAT SHIELD ENVIRONMENTS

The heat shield will be exposed to a wide range of environments from pre-launch through powered and space flight and finally during the brief but very intense entry heating period and subsequent subsonic descent in the planet's atmosphere. Figure 2 summarizes the environments imposed on the heat shield during each mission phase. These environments were used in the selection of the type of test and test conditions for characterizing the heat shield material.

The launch environments depicted in Figure 2 are from the published Shuttle payload bay design environments. Peak accelerations of up to 3.0 g_E's are expected during launch, but these are relatively insignificant compared to the 800 g_E's expected during steep entry into the Saturn/Uranus cold atmosphere. The launch acoustic and vibration environments are also relatively mild for the heat shield and will be a part of the engineering model vibration tests planned under SR&T Task 4.4.1.

During interplanetary flight, the heat shield will be subjected to hard vacuum for trip times of three to seven years. Previous flight experience indicates little if any degradation in strength or thermal properties of phenolic based materials exposed to hard vacuum. The heat shield will be inside the multilayer insulation blanket which together with the Radioisotope Heater Units (RHU's) will prevent excessive temperature excursions.

The most severe environments will be encountered during the brief deceleration time in the planet's atmosphere. The probe will enter at speeds that are about three to five times greater than any previous entry vehicle and will encounter a substantial amount of shock layer radiative heating in addition to the convective heating input. Figure 3 illustrates the peak heating and pressure environments in parametric form for a wide range of outer planet entry conditions and atmospheric models obtained from Reference 5. Figures 4 and 5 present heat flux time histories for Saturn and Jupiter entries and illustrate the large component of radiative heating present, especially for the higher speed Jupiter entries. The forebody heating distribution, shown in Figure 5, is relatively uniform over the entire body for the baseline 60° half-angle cone configuration (Reference 6). In general, peak heat fluxes of up to 50 Kw/cm^2 are predicted for a typical Jupiter entry and up to 25 Kw/cm^2 for a critical Saturn entry. Previous missile heating experience with carbon phenolic heat shields has been limited to about 20 Kw/cm^2 (missile nose tip heating has been higher but is less applicable to the probe environment) but this experience has been in a convective heating environment only. Current plasma arc facilities can provide only about 3.0 Kw/cm^2 of radiative heating (argon lamps) but the pilot arc facility currently in the final assembly phase at NASA-ARC will provide higher radiative heating rates with the proper hydrogen/helium gas mixtures.

The response of the heat shield to the intense Saturn and Jupiter environment is shown in Figures 6 and 7, respectively. A substantial amount of heat shield material is consumed during entry, especially for a Jupiter entry. Most of the recession is due to thermochemical (sublimation) processes but some

ENVIRONMENT \ MISSION PHASE	LAUNCH	SPACE FLIGHT	HYPERSONIC ENTRY		SUBSONIC ENTRY	
			JUPITER	SATURN/ URANUS	JUPITER	SATURN/ URANUS
TEMPERATURE – ^{o}C	4 TO 71	–40 TO 15	–40 TO 4200	–40 TO 4200	–73 TO 540	–73 TO 540
PEAK HEATING RATE $\frac{kw}{cm^2}$	–	–	40. TO 70.	6 TO 45	–	–
TOTAL HEAT – $\frac{kj}{cm^2}$	–	–	250 TO 400	60 TO 100	–	–
PRESSURE – ATM	1.0 TO VAC	VACUUM	VAC TO 12	VAC TO 20	0.1 TO 30	0.1 TO 10
PEAK DECELERATIONS – g_E's	3.0*	–	200 TO 400	100 TO 800	–	–
ACOUSTICS – db	135*	–	–	–	–	–
VIBRATION – g^2/Hz	0.07*	–	–	–	–	–

*SHUTTLE PAYLOAD BAY ENVIRONMENTS

FIGURE 2
HEAT SHIELD ENVIRONMENT

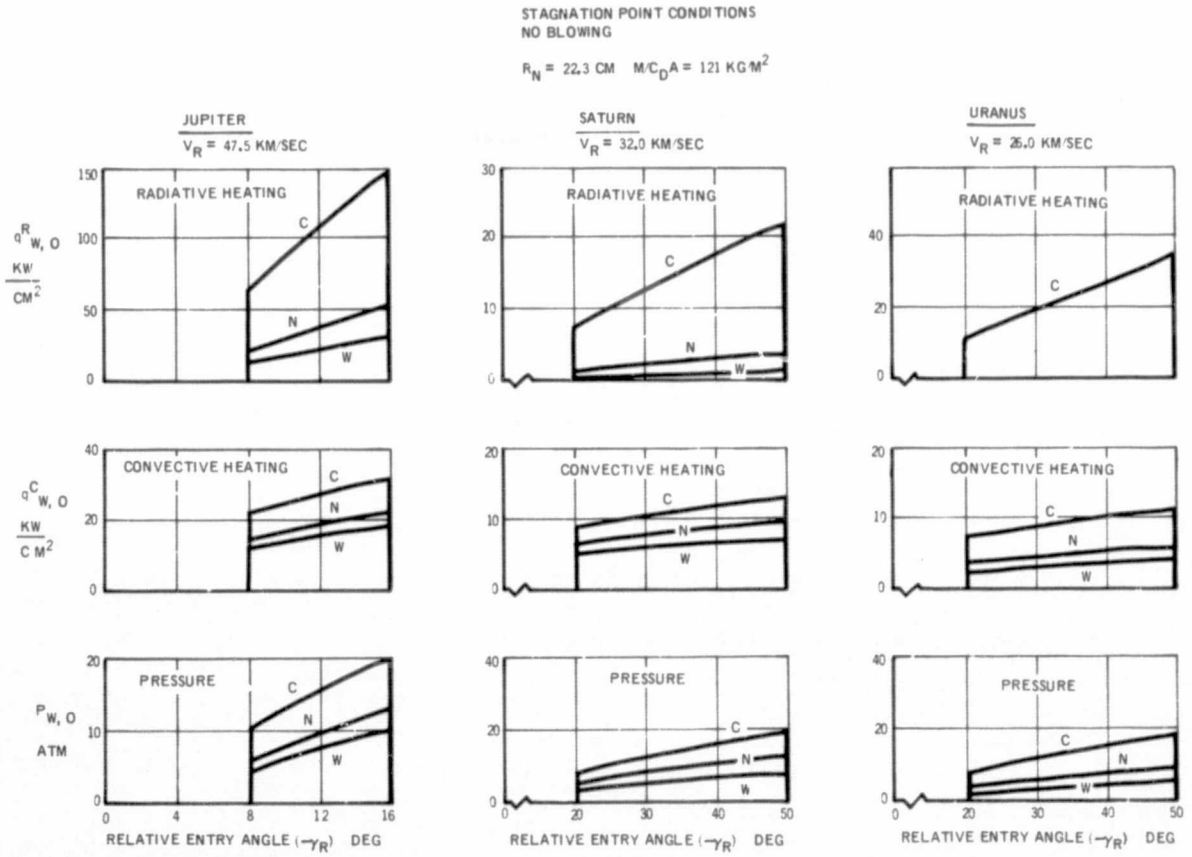

FIGURE 3
OUTER PLANET PEAK ENTRY ENVIRONMENTS

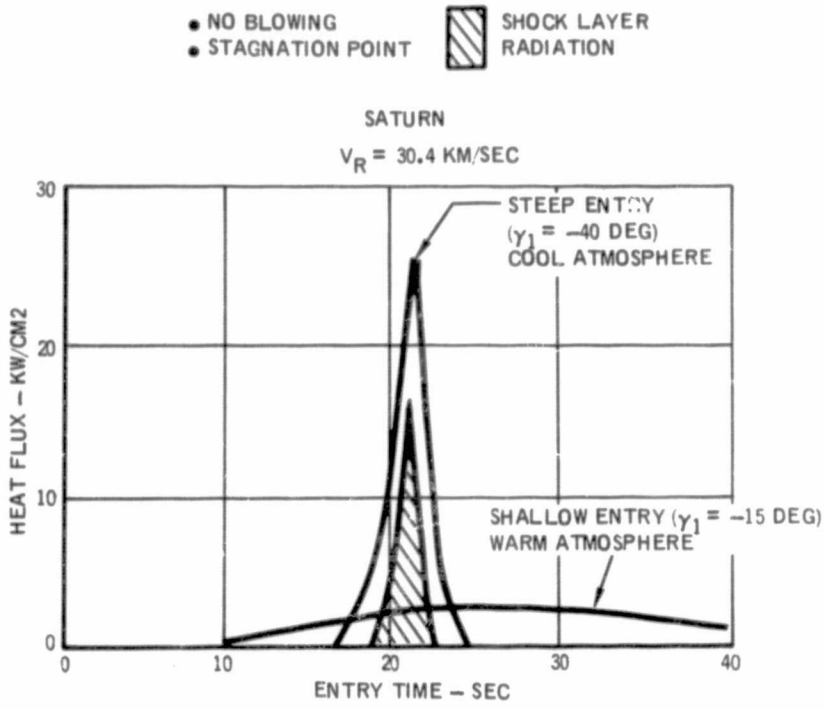

FIGURE 4
SATURN ENTRY HEATING ENVIRONMENT

mechanical erosion has been conservatively assumed and estimated from empirical correlations based on missile flight data. Although relatively high recession rates are predicted for a Jupiter entry, the estimates are within the recession rates measured on various missile programs. The temperature gradients on heat shields experiencing high recession rates are very steep but the heated zone is confined within a very thin layer near the surface. Thus, the material below the heated zone remains at the initial temperature until it senses the receding surface. The point to be made is that even though a substantial difference in the external environment exists between planetary heating and previous missile entry experience, the heat shield response in terms of recession rates, temperature gradients, pyrolyses mass flow rates and pressure gradients is very similar and this data base provides the confidence for a successful probe entry.

The combination of a large heat shield exposed to relatively high aerodynamic pressures and temperature gradients results in significant internal stresses on the remaining uncharred heat shield. Stress analyses of the uncharred portion of the heat shield have been performed at peak entry heating and at peak aerodynamic loading. The limit stresses in the uncharred heat shield and at the adhesive bondline predicted for the two critical entry conditions are presented in Figure 8. These stresses are within the strength capability of the heat shield material and of the adhesive bond.

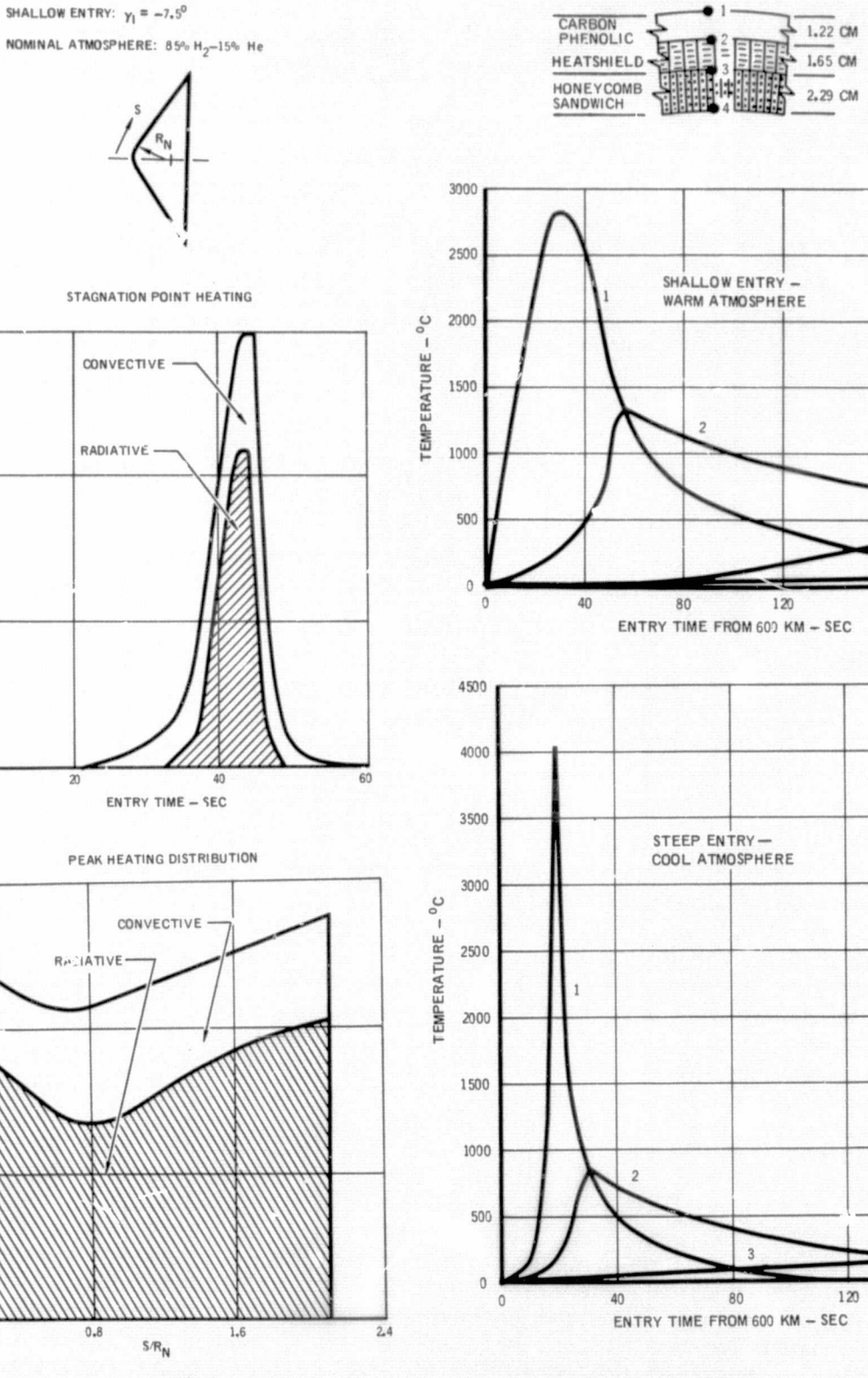

FIGURE 5
JUPITER ENTRY HEATING ENVIRONMENT

FIGURE 6
SATURN HEAT SHIELD THERMAL RESPONSE

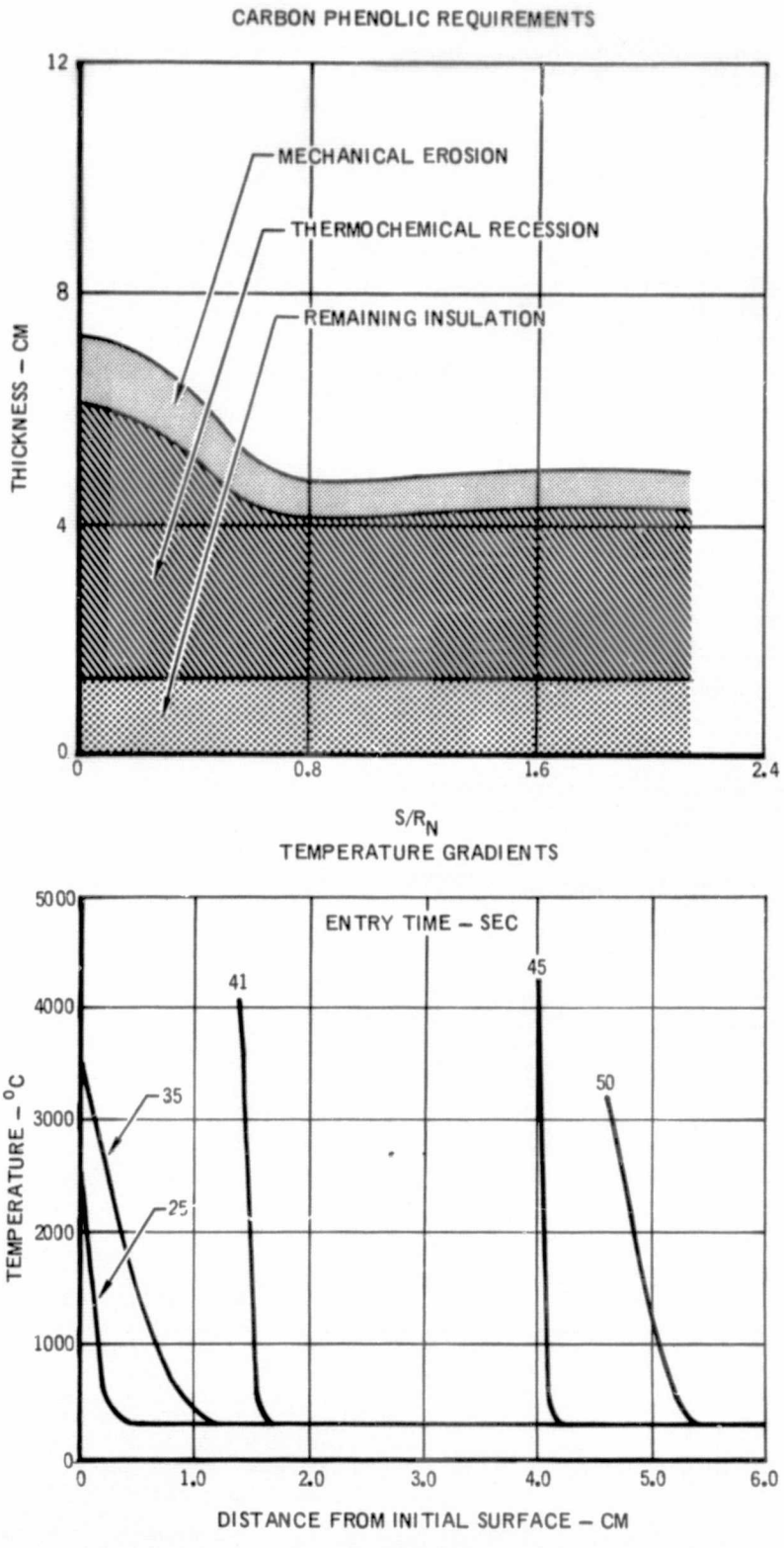

FIGURE 7
JUPITER HEAT SHIELD RESPONSE

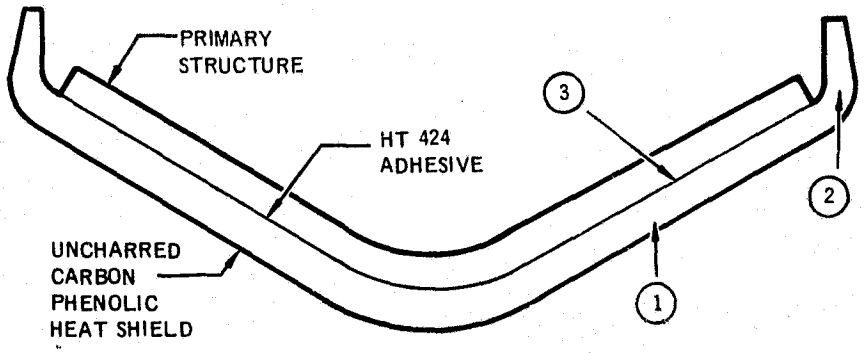

CROSS SECTION

MATERIAL	LOCATION	LOAD CONDITION	ULTIMATE STRESSES	
			CROSS LAMINAR TENSION MN/m^2	INTERLAMINAR SHEAR MN/m^2
CARBON PHENOLIC	(1)	1	1.82	4.58
CARBON PHENOLIC	(1)	2	3.00	6.20
CARBON PHENOLIC	(2)	2	11.0	1.54
HT 424	(3)	1	–	1.68
HT 424	(3)	2	–	2.08

FIGURE 8

MAXIMUM ULTIMATE STRESSES – JUPITER HEAT SHIELD

The heat shield is retained throughout the atmospheric descent phase and its temperature will eventually approach the temperature of the atmosphere. Figure 9 depicts the heat shield temperatures and pressures during descent to the 30 BAR pressure level. During the terminal descent phase when mass spectrometer measurements are made, the heat shield continues outgassing at a diminishing rate. Some of the outgassing products are identical to the trace constituents of the atmosphere and must not be ingested in the mass spectrometer sample. Previous experiments (Reference 7) have demonstrated that by extending the sampling inlet tube sufficiently forward of the heat shield surface heat shield contaminants can be avoided. Additional testing and development work on the inlet extension system is addressed by SR&T Task 4.3.3.

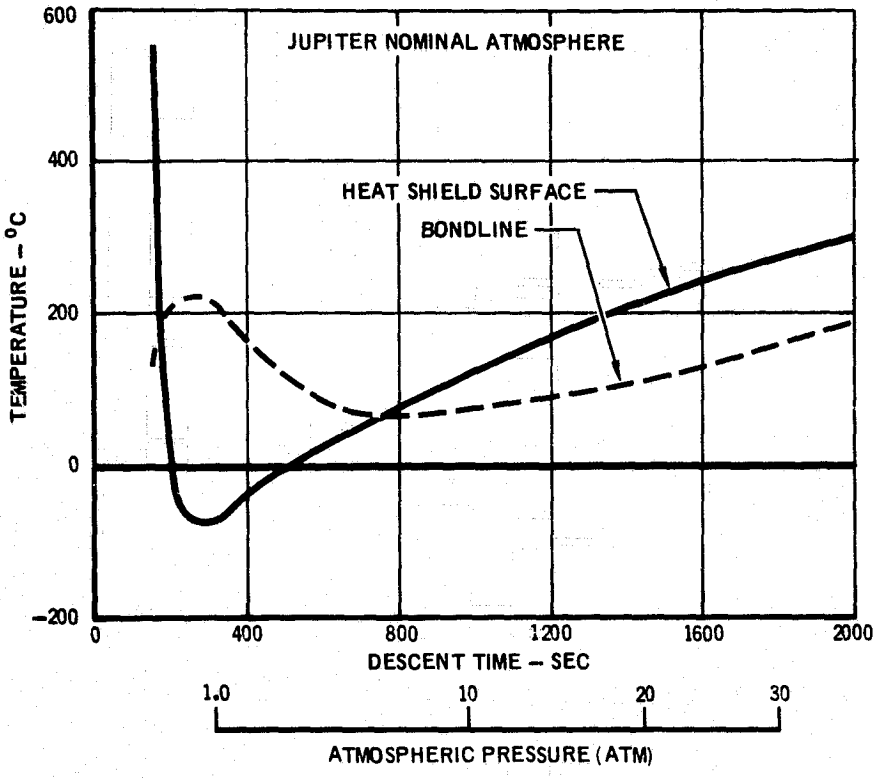

FIGURE 9

HEAT SHIELD TEMPERATURES DURING DESCENT

PROBE HEAT SHIELD CHARACTERISTICS

Maximizing commonality of the probe and its subsystems is a desired goal for minimizing program costs in the exploration of the three outer planets. Commonality of the forebody heat shield is achieved by using the same material (carbon phenolic), probe shape (60° sphere-cone), cloth orientation, and heat shield fabrication method; however, in order to minimize weight the heat shield thickness will be tailored to the requirements of each mission.

Heat Shield Configuration - Figure 10 depicts the heat shield configuration for either the Saturn/Uranus or Jupiter mission. Both heat shield designs are based on the same external mold shape and both incorporate two plugs in the heat shield that are penetrated with the atmospheric sampling and temperature measurement instruments. The SUAEP heat shield is approximately 2.9 cm thick, with the inner 1.6 cm portion of the heat shield hollowed-out to reduce weight. The Jupiter heat shield is approximately 5.0 cm thick and solid. It is not hollowed-out in order to provide additional conservatism.

Even though the SR&T work was to emphasize the Jupiter mission, ARC and MDAC mutually agreed that building the SUAEP heat shield was cost effective in that the heat shield could subsequently be used in the engineering model test program. In terms of fabrication complexity, building the thicker Jupiter heat shield is not considered significantly more difficult. As shown in the heat shield cross-section comparison presented in Figure 11, fabrication of the Jupiter heat shield requires one additional processing step and wider prepreg rings than the SUAEP heat shield.

Ply Orientation Requirements - A composite material such as carbon phenolic consists of a reinforcement (carbon cloth) and a binder (phenolic). It is desirable if not essential that the reinforcement be continuous from the bondline to the surface in order to prevent loss of plies. In addition, the ply direction must be at least 10° above the surface plane so that the ablation gases may flow to the surface between plies rather than across, thus preventing excessive internal pressure build-up. A 20° lay-up is commonly used and represents an optimum trade between material conductance (increases with higher ply angle) and internal pressure build-up (increases with lower ply angle). Ply angles above 20° are permissible but lower ply angles are to be avoided.

As shown in Figure 1, if the horizontal lay-up used to form the cone was continued in the nose cap area, it would have led to a 0° lay-up near the apex of the nose cap, which is undesirable. The multistep method permits bending and orientating the nose cap plies so that the proper ply angle is maintained (Figure 1) and also allows fabrication of the hemispherical nose cap and cone frustrum as one integral unit.

In the cone frustrum, the ply orientation is a natural 30° and results from the combination of a horizontal prepreg lay-up coupled with a 60° half-angle cone frustrum. The higher cloth angle (30° vs 20°) imposes a slightly higher thermal conductivity penalty but greatly simplifies the fabrication process.

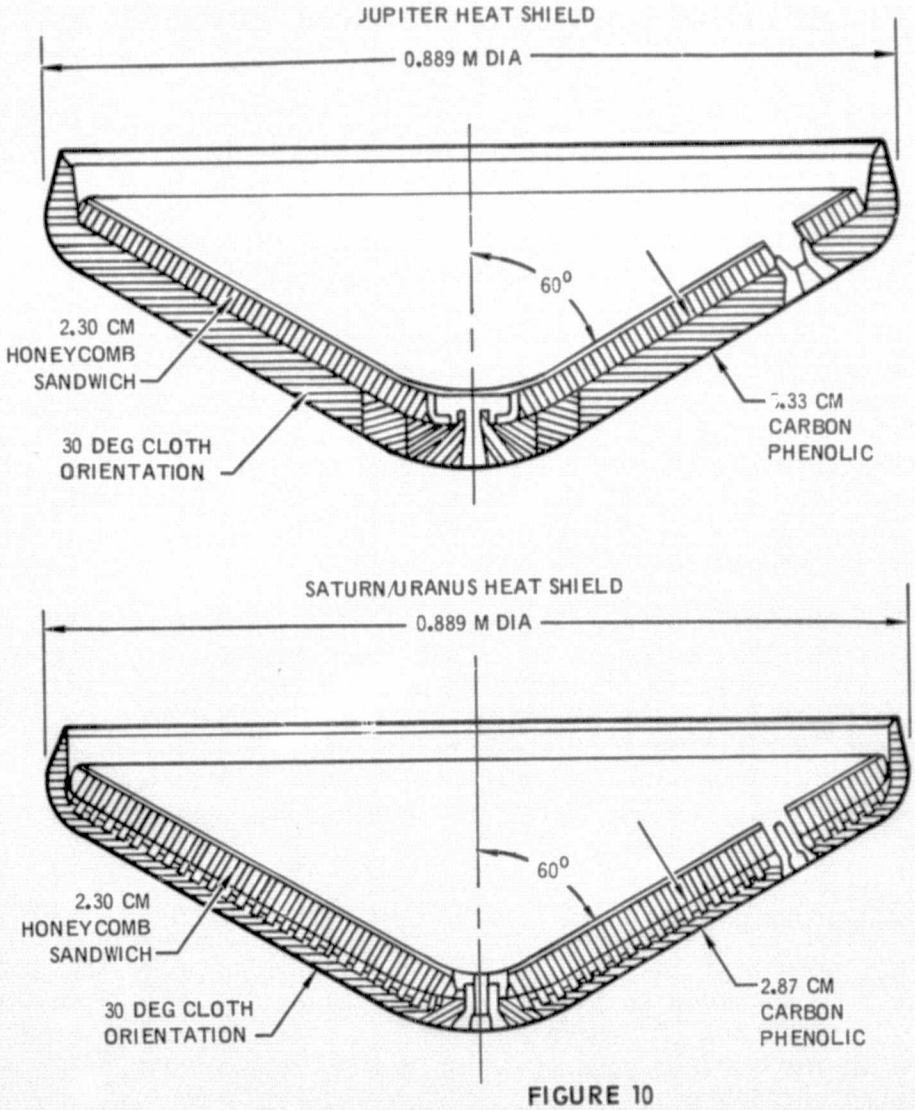

FIGURE 10
OUTER PLANET PROBE HEAT SHIELD CONFIGURATION

Continuation of the horizontal lay-up around the base corner results in an increase in ply orientation from 30° to 90°. Ideally, it would have been desirable to maintain a lower ply angle around the base corner. However, bending the plies over the small turning radius of the base corner would have greatly complicated the fabrication procedure and was therefore not attempted on the present heat shield. The 90° orientation results in a conductivity that is perhaps 50% higher than the 20° lay-up and must be factored into the sizing analyses; however, the 90° lay-up does not have the potential catastrophic problem of excessive pressure build-up associated with the 0° lay-up that mandated a change in the nose cap ply orientation.

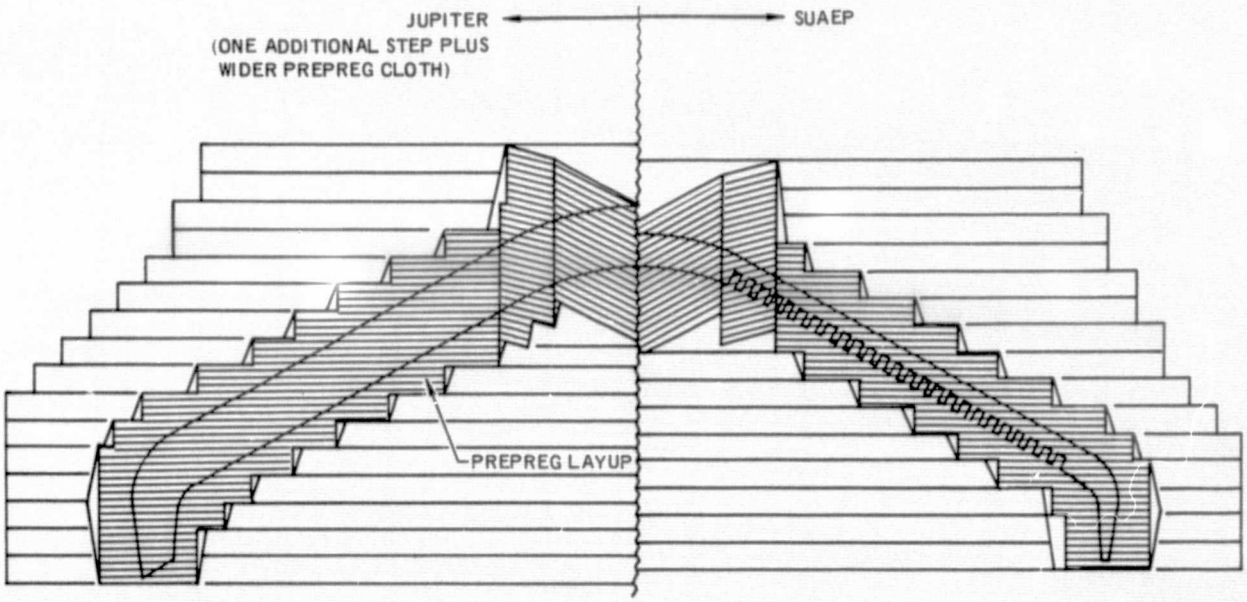

FIGURE 11

FABRICATION COMPARISON BETWEEN JUPITER AND SUAEP HEAT SHIELDS

HEAT SHIELD FABRICATION

Fabrication of the full scale carbon phenolic heat shield was the major activity of this SR&T task. The major steps in the fabrication effort are summarized below and discussed in this section:

- o A survey of candidate prepreg materials was conducted leading to selection of the Fiberite MX 4910HP prepreg.
- o Preliminary processing evaluations were made with small stacks of prepreg to characterize the new prepreg material and determine the pressure-temperature-time cure profile.
- o A short two-step stack, representative of the actual heat shield, was built using full scale tooling.
- o Circular prepreg rings and discs were cut from the rolls of prepreg bought from Fiberite Corp. and assembled into 15 stacks each containing 68 plies.
- o A full scale heat shield stack was assembled by the multistep method and cured to form the carbon phenolic billet.
- o The billet was machined to the Saturn/Uranus heat shield configuration.

Prepreg selection.- Because new prepreg materials are continuously evolving and previously used prepreg materials are no longer in production, a survey of currently available prepreg materials was conducted. The survey centered on evaluating the prepreg materials produced by the two fabricators: U.S. Polymeric and Fiberite. Figure 12 presents property data on available prepreg materials and also for Fiberite's MXC-31 (previously used on classified missile programs) which will serve as a reference for comparison. In general, the variation in property data between materials is relatively small, especially considering that the measurements were made at different laboratories. Based on these data and inputs from the vendors and DOD personnel involved in the missile heat shield technology programs at the Air Force Wright Patterson Material Laboratory and at Aerospace Corporation (References 4 and 5) the selection of prepreg was reduced to the best material from each vendor: namely, the Fiberite MX 4910HP and the U.S. Polymeric FM 5056A prepreg. Both of these prepregs use HITCO's CCA-2(1641) carbon cloth. In order to make the final selection, prepreg was obtained from each vendor and carbon phenolic blocks were fabricated at MDAC. Thermal (oxy-acetylene and conductivity) and mechanical (flexure) tests were conducted with specimen cut from these blocks and the results presented in Figure 13 show that within the accuracy of the measurements, the performance of both materials is similar. Figure 14 lists some of the pertinent factors considered in the final prepreg selection process. Fiberite's MX 4910HP prepreg was selected for fabrication of the full scale heat shield principally on the basis that the phenolic resin, Monsanto SC 1008, is identical to the resin employed in the MXC-31 prepreg which we have worked with in the past and are most familiar with its processing characteristics.

Manufacture of prepreg: Figure 15 is a flow diagram of the steps and manufacturers involved in making the selected carbon phenolic prepreg. The process begins by forming the continuous rayon yarn. The rayon yarn is woven into cloth and carbonized by heating in an inert environment. The carbon cloth is then

PROPERTY	UNITS	PLUTON FIBERITE (MXC-31)	FIBERITE (MX-4910-HP)	U. S. POLY (FM 5056A)	U.S. POLY (FM 5056)
RESIN CONTENT	PERCENT	42.5	37.6	35.3	34.5
SPECIFIC GRAVITY	GM/CM^3	1.4	1.47	1.46	1.46
TENSILE STRENGTH	MN/M^2	94.5	120.7	137.2	154.5
TENSILE MODULAS		11721.0	15850.0	18610.0	19650.0
FLEXURAL STRENGTH		137.9	185.5	233.0	242.0
COMPRESSIVE STRENGTH		230.9	272.4	286.8	355.8
INTERLAMINAR SHEAR		35.2	21.0	20.1	17.2
FLATWISE TENSILE		31.0	8.3	8.0	11.9
BARCOL HARDNESS		–	74	74	75
SPECIFIC HEAT	$CAL/GM-^oK$	0.25	0.27	0.25	0.23
THERMAL CONDUCTIVITY	$W/M-^oK$	0.76	0.97	0.97	0.86
REFERENCE		SRI	GE	GE	USP

FIGURE 12
CARBON PHENOLIC PROPERTY DATA

PROPERTIES \ PREPREG	U.S. POLYMERIC FM 5056A	FIBERITE MX 4910HP
• OXY-ACETYLENE TORCH TEST FOR 30 SEC		
– SURFACE TEMPERATURE ^oC	2120	2130
– RECESSION – CM	0.03	0.03
– WEIGHT LOSS – GRAMS	1.35	1.39
• SPECIFIC GRAVITY	1.54	1.49
• THERMAL CONDUCTIVITY – $W/m-^oK$	0.74	0.68
• FLEXURAL STRENGTH – 10^6 N/m^2	262	248

FIGURE 13
IN-HOUSE PREPREG SCREENING TEST RESULTS

impregnated with pehnolic resin that includes 10% carbon black and "B"-staged. "B"-staging involves oven heating the prepreg to drive-off the low molecular weight volatiles and the isopropyl alcohol that was the solvent for the phenolic resin in the impregnation process. Partial polymerization of the phenolic resin occurs during heating which increases the stiffness and reduces the tackiness of the prepreg cloth. The multistep method requires a prepreg with high drapability, in order to form the double inversed chevron nose cap plies, and a relatively long working life to permit assembly of the heat shield stack. To meet our requirements of higher drapability and longer working life, Fiberite was directed to "B"-stage the material at 90°C for 30 minutes - a cycle that is lower than the "B"-stage level normally used by Fiberite. "B"-staging at the lower temperature provided the option of additional inhouse "B"-staging at a later date. The lower "B"-staged prepreg had an 11% volative content which is twice the content normally obtained. (The prepreg was procured from Fiberite per McDonnell Douglas Material Specification MMS 517.)

• VENDOR	FIBERITE	U. S. PLOYMERIC	COMMENTS
• CANDIDATE PREPREG	MX 4910HP	FM 5056A	
• CARBON CLOTH	HITCO'S CCA-2 (1641)-10		AM. ENKA TO STOP PRODUCTION, AM. VISCOSE RAYON BEING EVALUATED
• PHENOLIC RESIN	MONSANTO'S SC1008 CTL 91LD (MOD.)		
• PUBLISHED DATA			
MECHANICAL PROPERTIES	SIMILAR		
THERMAL PROPERTIES	SIMILAR		
THERMAL PERFORMANCE	SIMILAR		
• MDAC DATA			
MECHANICAL PROPERTIES	SIMILAR		
THERMAL PERFORMANCE	SIMILAR		
• PROCESSING INFORMATION			
RESIN FLOW	VERY LOW (GOOD)	VERY HIGH	AFML STATED THAT FM5056A IS HARDER TO CONTROL
PROCESSING	OK	OK	
• FLIGHT DATA	YES	YES	
• SELECTED MATERIAL			MDC HAS EXPERIENCE WITH THIS RESIN SYSTEM

FIGURE 14

CARBON PHENOLIC PREPREG SELECTION

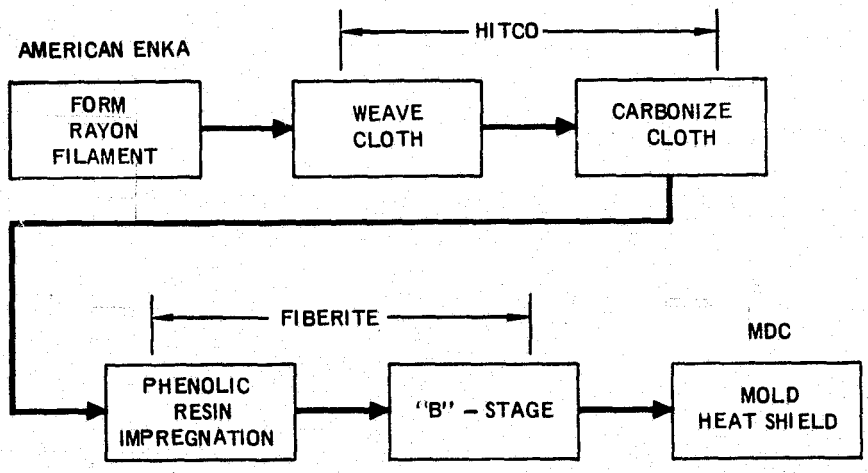

FIGURE 15

PROCESSIGN OF CARBON PHENOLIC PREPREG

Preliminary processing work. - Initial processing work was performed with small stacks of prepreg with the objective being determination of the process variables (primarily the temperature, pressure, time cure cycle) required for multistep fabrication. This effort was required because:

(1) A new prepreg (MX 4910HP) was used that was considerably "greener" and less advanced than previous prepregs.

(2) Scale-up or process development monies were not available and the high cost of the prepreg dictated a "one-shot" successful attempt at making the full scale heat shield.

Prepreg debulking. - Assembly of the heat shield and tooling stack by the multistep method requires debulking the prepreg within the tooling step thickness (2.5 cm). The pressure and temperature required to properly debulk the prepreg plies was evaluated by experimenting with small stacks of plies. At room temperature, an 80 ply stack (10 cm x 10 cm) was initially 5.0 cm high in the uncompressed state and could be compressed to 3.3 cm with 34 atm; however, after removal from the press the stack would eventually regain its original height. Raising the stack temperature from room temperature to 52°C and then compressing did not greatly alter the spring-back history. Raising the temperature above 52°C and pressing resulted in excessive resin flow (loss). Compressing at room temperature at 20 to 34 atm followed by rapid cooling to about -18°C significantly delayed the spring-back movement to less than .50 cm over an 18 hour period. Subcooling the prepreg layers increases the viscosity of the resin to almost a solid state and this physical force retains the prepreg layers.

Prepreg resin characteristics. - While compressing the stack of prepreg layers, it was noticed that resin began to flow at temperatures above 52°C. Resin flow at this relatively low temperature range was not expected and was attributed to the lower "B"-staging temperature history of the prepreg.

Temperature, pressure, duration and previous conditioning history all affect resin flow. Increasing the prepreg temperature decreases the visocity, which promotes resin flow, but increases the polymerization rate, which inhibits resin flow. Increasing pressure, in general will promote resin flow. Increasing the duration at temperature will decrease resin flow (increases polymerization). The extent of prior "B"-staging strongly affects resin flow. Minimization of resin loss requires selection of the proper "B"-staging level and the proper pressure-temperature-time profile that is also compatible with the fabrication requirements.

Figure 16 presents some of the resin flow/volatile loss characteristics of the MX 4910HP prepreg. Figure 17 depicts the strong influence temperature has in the removal of the volatile constituents. The figure also presents resin flow data from a standard test performed by first exposing prepreg plies at the temperatures and durations shown then compressing the plies with 68 atm of pressure and measuring the amount of resin squeezed-out of the material. The working life of the material is indicated by the resin loss approaching zero, i.e., the resin has completely polymerized. The working life for the MX 4910HP prepreg is at least 8 hours at 60°C which is sufficient time to assemble the heat shield by the multistep method.

Cure cycle determination. - Small stacks of prepreg 10 cm x 10 cm x 2.5 cm thick and 15 cm x 30 cm x 2.5 cm thick, representative of a portion of a step, were processed to determine the pressure-temperature-time profile (Figure 17). In the first few runs, excessive resin flow was evident at about 68°C. This problem was solved by further "B"-staging the prepreg at 65°C for 30 minutes and by heating the prepreg at about 60°C for 8 hours (see Figure 17) in the

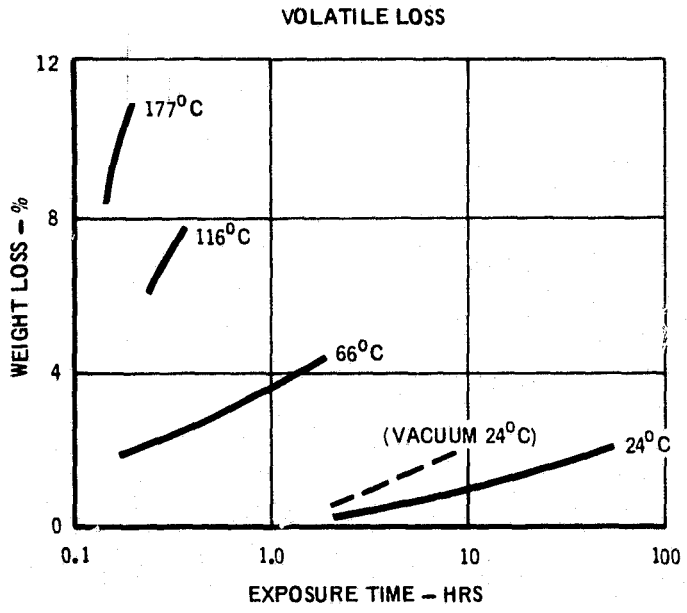

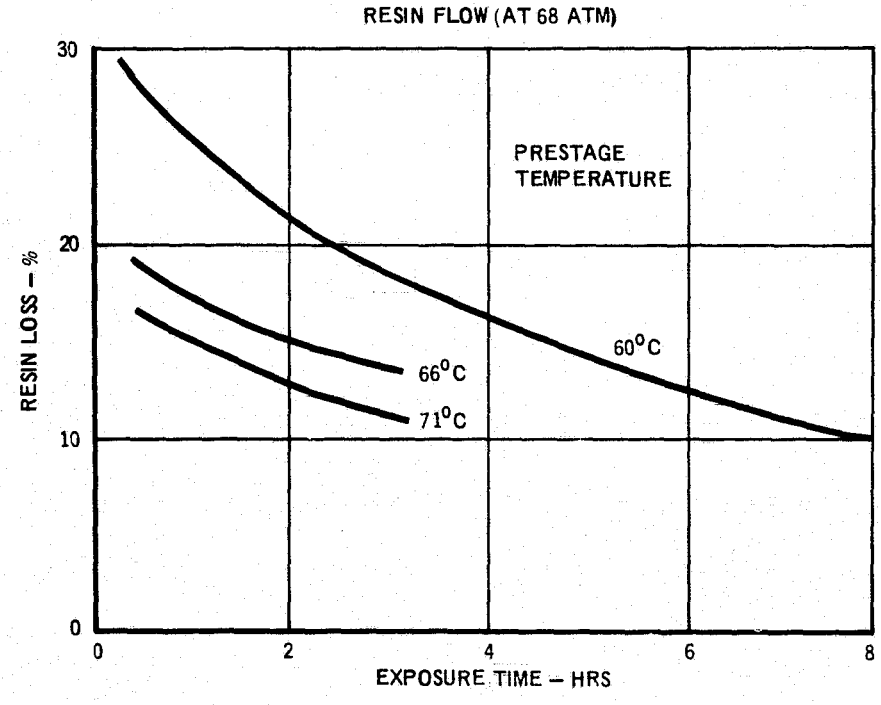

FIGURE 16

PREPREG RESIN LOSS CHARACTERISTICS

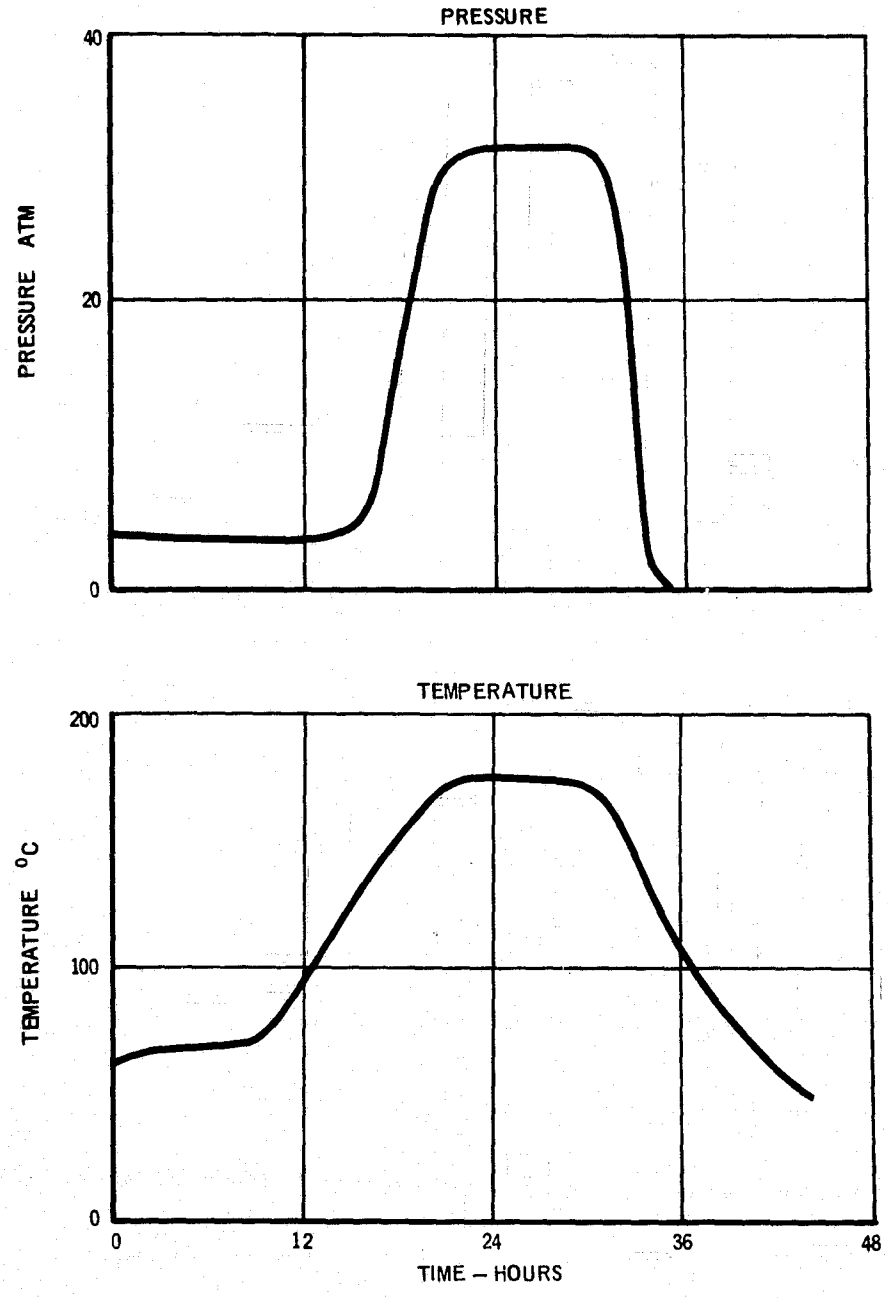

FIGURE 17
CURE CYCLE ESTABLISHED BY PRELIMINARY PROCESSING WORK

press prior to increasing the temperature up to 65°C and finally to 177°C for final cure. Low temperature heating of the phenolic resin, increases the polymerization of the resin (i.e., long molecular chains are formed), increases the resin viscosity and thus prevents resin flow. The last two test blocks were judged to be good as evidenced by minimum resin loss, attainment of the proper density and the lack of any voids or delaminations. The number of plies required to achieve 2.5 cm of solid carbon phenolic thickness for the last two blocks were computed to be 70.9 (small resin flow) and 68.5 (almost no resin flow).

Subassembly process demonstration. - Prior to fabricating the full scale heat shield, a short stack, Figure 18, consisting of the two-steps near the nose cap-cone tangency line were processed utilizing full scale tooling and 70 plies of prepreg per step. A cross-sectional cut of the formed part, Figure 19, revealed the presence of cracks on the inside area of the lower step. These cracks were unbonded plies caused by insufficient pressure transmitted to the part during curing. Mismatches in the nose cap tooling (only the nose cap tooling was machined; the rest of the tooling was cut from flat plate stock) produced excessive loading in the inverse chevron region and insufficient pressure on the sides where the cracks were found (see Figure 20). The tooling was corrected by additional machining and the number of prepreg plies adjusted prior to full scale fabrication.

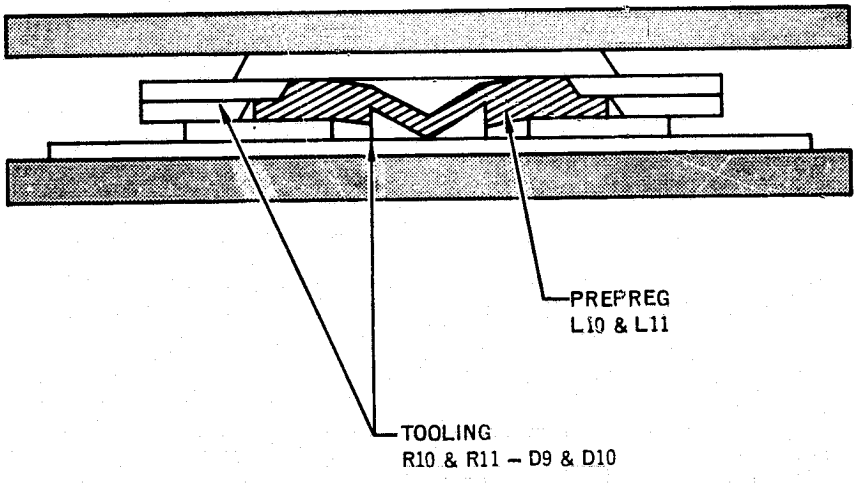

FIGURE 18
TWO-STEP HEAT SHIELD FABRICATION

Full scale fabrication.

Cutting of prepreg rings. - The prepreg material purchased from Fiberite Corp. was delivered in 107 cm wide rolls containing 91 meters of material. The prepreg was spread on a flat table, covered on both sides with plastic film and hand-cut into circular prepreg rings or discs (for nose cap) with the aid of

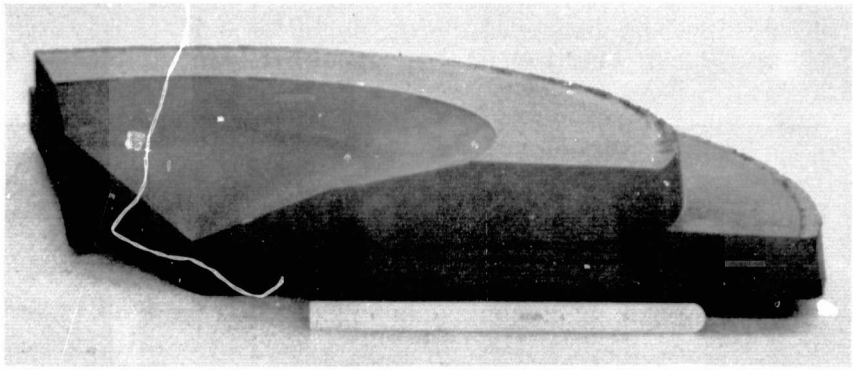

FIGURE 19

CROSS-SECTION OF TWO-STEP HEAT SHIELD BILLET

FIGURE 20

CUTTING OF PREPREG PLIES

aluminum templates (Figure 20). A total of 80 plies were cut for each of the 15 steps. The dimensions of the prepreg plies and of the tooling components are presented in Figure 21. In most cases the smaller rings were cut from material remaining after cutting the larger rings (Figure 22); thus, prepreg utilization was maximized to about 75%. At all times, except in the cutting operation, the prepreg was refrigerator stored at 4°C to prevent further polymerization of the phenolic resin.

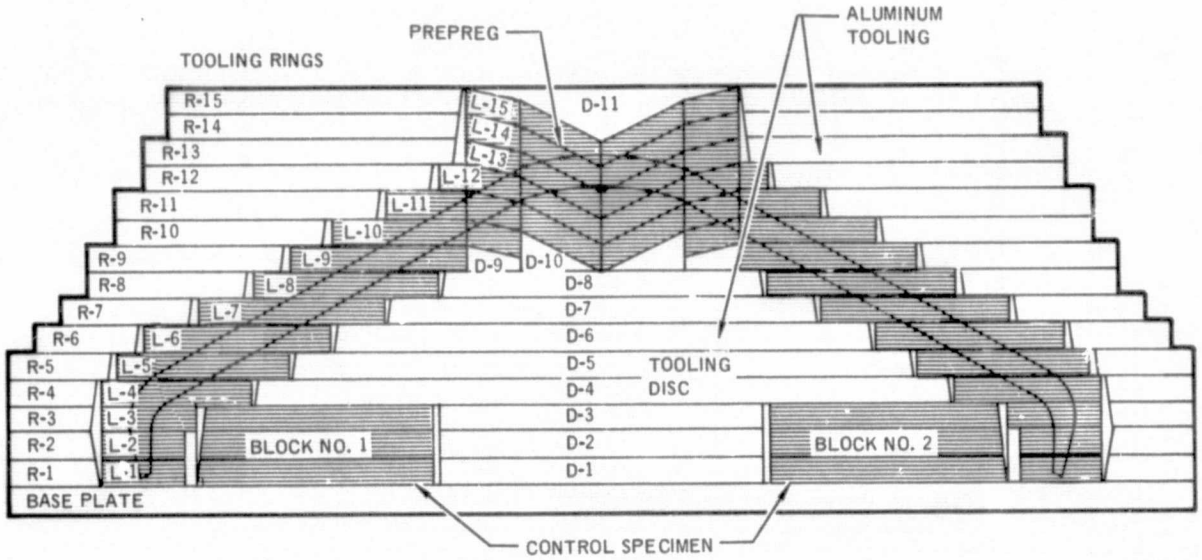

DIMENSIONS – CM

	PREPREG		OUTER TOOLING RINGS			INNER TOOLING DISC		
	ID	OD		ID	OD		ID	OD
L1	78.7	94.0	R1	94.6	111.8	D1	78.7	0
L2	78.7	94.0	R2	94.4	111.8	D2	78.1	0
L3	76.2	94.0	R3	94.6	111.8	D3	75.6	0
L4	66.0	94.0	R4	94.6	111.8	D4	65.4	0
L5	58.4	91.4	R5	92.1	111.8	D5	57.8	0
L6	50.8	86.4	R6	87.0	106.7	D6	50.2	0
L7	40.6	76.2	R7	76.8	101.6	D7	40.0	0
L8	30.5	66.0	R8	66.7	96.5	D8	29.8	0
L9	25.4	58.4	R9	59.0	96.5	D9	25.4	15.2
L10	15.2	50.8	R10	51.4	91.4	D10	15.2	0
L11	0	40.6	R11	41.3	91.4	D11	25.4	0
L12	0	30.5	R12	31.1	86.4			
L13	0	25.4	R13	27.3	86.4			
L14	0	25.4	R14	26.7	81.3			
L15	0	25.4	R15	26.0	81.3			

FIGURE 21
PREPREG PLIES AND TOOLING IDENTIFICATION

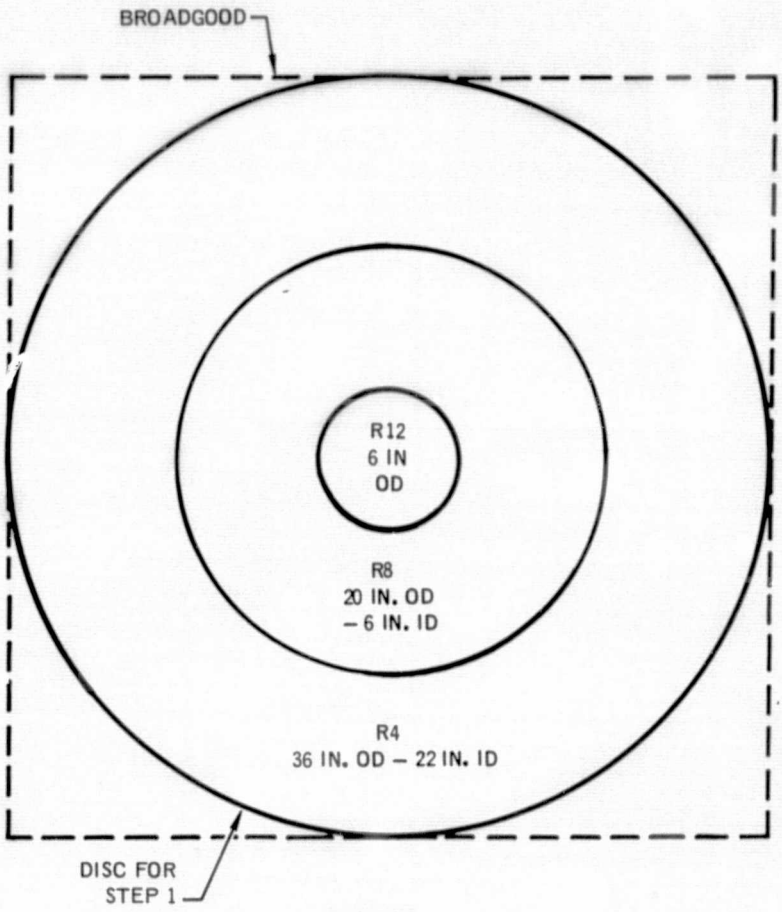

FIGURE 22
EFFICIENT UTILIZATION OF PREPREG

Preparation of prepreg plies. - The preliminary processing work with small stacks indicated that additional "B"-staging was required to avoid resin flow during processing. This was accomplished by placing the prepreg in an air circulating oven and heating the material at 66°C for 30 minutes. The plies were then stored in the cooler until needed.

The plies used in the nose cap area, Steps L-10 through L-15, were preformed to a double inverse chevron configuration (see Figure 21) to achieve the proper ply orientation. The plies were preformed by (1) softening the prepreg with the aid of a heat gun, (2) hand-stretching the plies in the bias direction of the fabric weave, and (3) placement of the plies in the shaped tooling and pressing to the proper shape. The shaped plies were cooled to room temperature which increased the stiffness of the material and helped in maintaining the ply shape.

In forming the sets of prepreg plies for each step, the plastic film protective layers were removed and each prepreg ply was rotated 45° from the previous ply as shown in Figure 23 to eliminate the bias direction of the cloth.

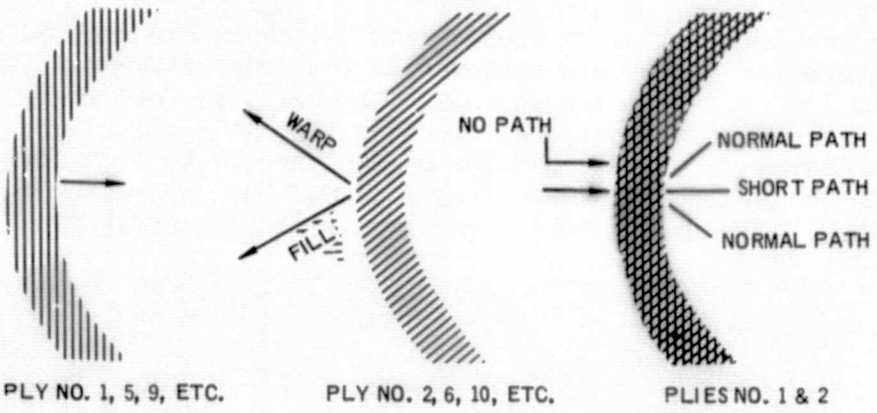

FIGURE 23
ROTATION OF PREPREG PLIES DURING LAYUP

Each set of ring plies (Sets L-1 through L-9) was debulked by compressing with 34 atm of pressure and at room temperature. The compressed ply sets were placed on a plywood ring of similar size, wrapped and returned to the 4°C cooler until heat shield assembly.

Assembly of the heat shield stack and tooling - After three years of limited subscale fabrication development and thinking about multistep molding, we were ready to initiate fabrication of the full scale probe heat shield. We knew from previous experience that the scale up to large masses would necessitate some modifications to our basic plan to react to unforseen events occurring during the processing operation. In the following paragraphs the fabrication sequence is briefly discussed and visually illustrated by the photographs taken at various points during fabrication. In describing the fabrication sequence, reference is made to Figure 21 that shows an overview of the stack assembly, and identifies the tooling and prepreg steps and Figure 24 which identifies the thermocouple locations.

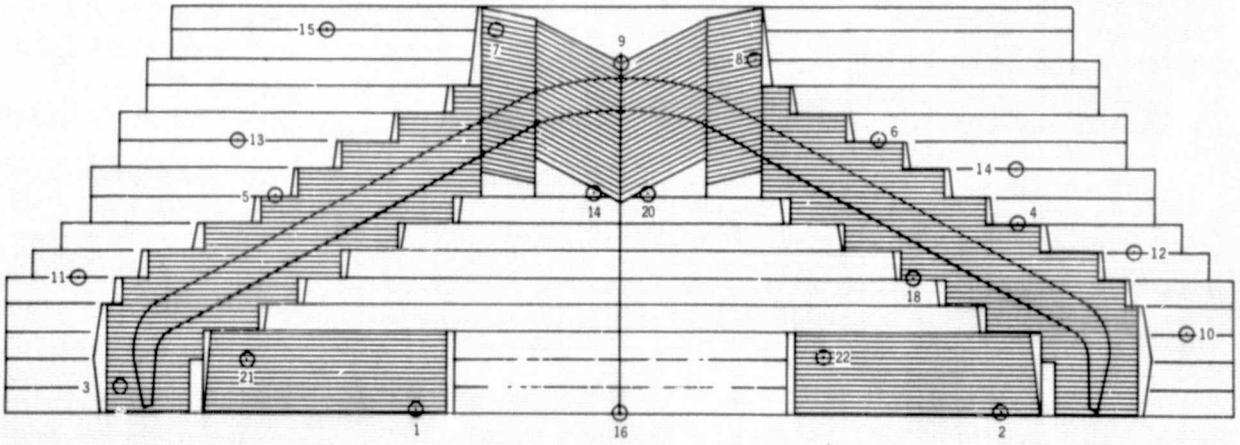

FIGURE 24
THERMOCOUPLE LOCATIONS

Twenty-four hours prior to heat shield build-up, the prepreg plies were removed from the 4°C cooler and returned to the temperature and humidity controlled room, Figure 25. The heat shield tool base, and bottom three internal tooling discs and the first external tooling ring were placed in the press (Figure 26), the press closed, and the platens heated to a uniform temperature of 60°C. All other tooling segments were placed in a nearby oven and also heated to 60°C for future use. The bottom three sets of prepreg rings and the plies

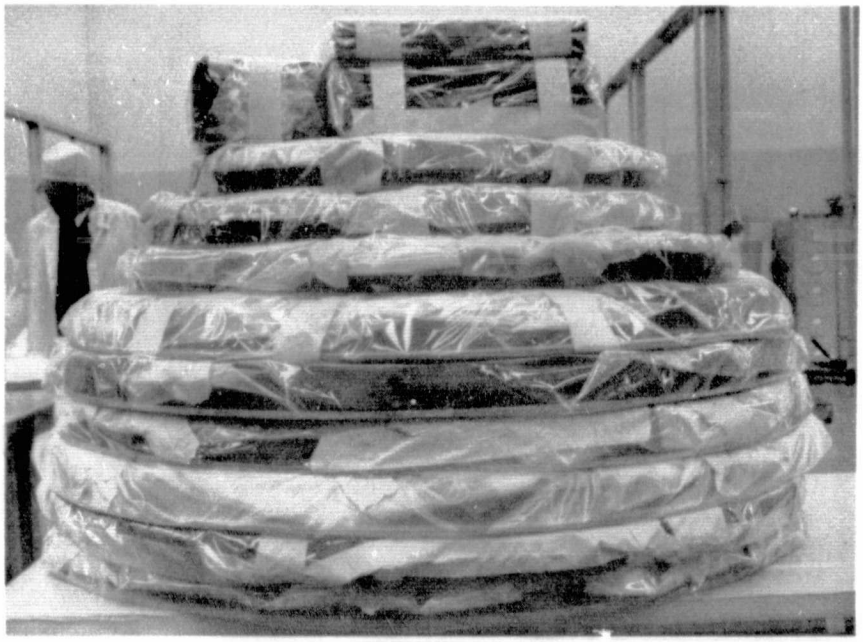

FIGURE 25

PREPREG STACK PRIOR TO ASSEMBLY

for the control specimen blocks were positioned into the preheated tooling as shown in Figure 26. All thermocouples (Figures 24 and 26) that would monitor the interior temperatures were installed through the lower tooling plates. The bottom three sets of plies have the same outside diameter and were therefore compacted in a single step operation. The press was then closed and a pressure of 34 atm was applied for 10 minutes to further reduce the prepreg bulk height.

At the time ply Sets L-1, L-2 and L-3 were placed in the hot platen press, ply Sets L-4 thru L-9 were placed in a 60°C oven, and ply Sets L-10 thru L-15 were assembled and placed in a separate small heated platen press. This was done so that all prepreg plies experience the same temperature history. Ply Sets L-10 thru L-15 included all of the preformed plies for the double inverse chevron nose cap portion of the heat shield.

At the end of the 10 minute debulking cycle for the first three sets of plies, the pressure was released, the press opened and the fourth set of plies was added with its appropriate tooling (Figure 27). One inch long dowel pins were added with each tooling segment to hold the tooling in place. The press was closed and pressure applied for the second debulking sequence. Ply Sets

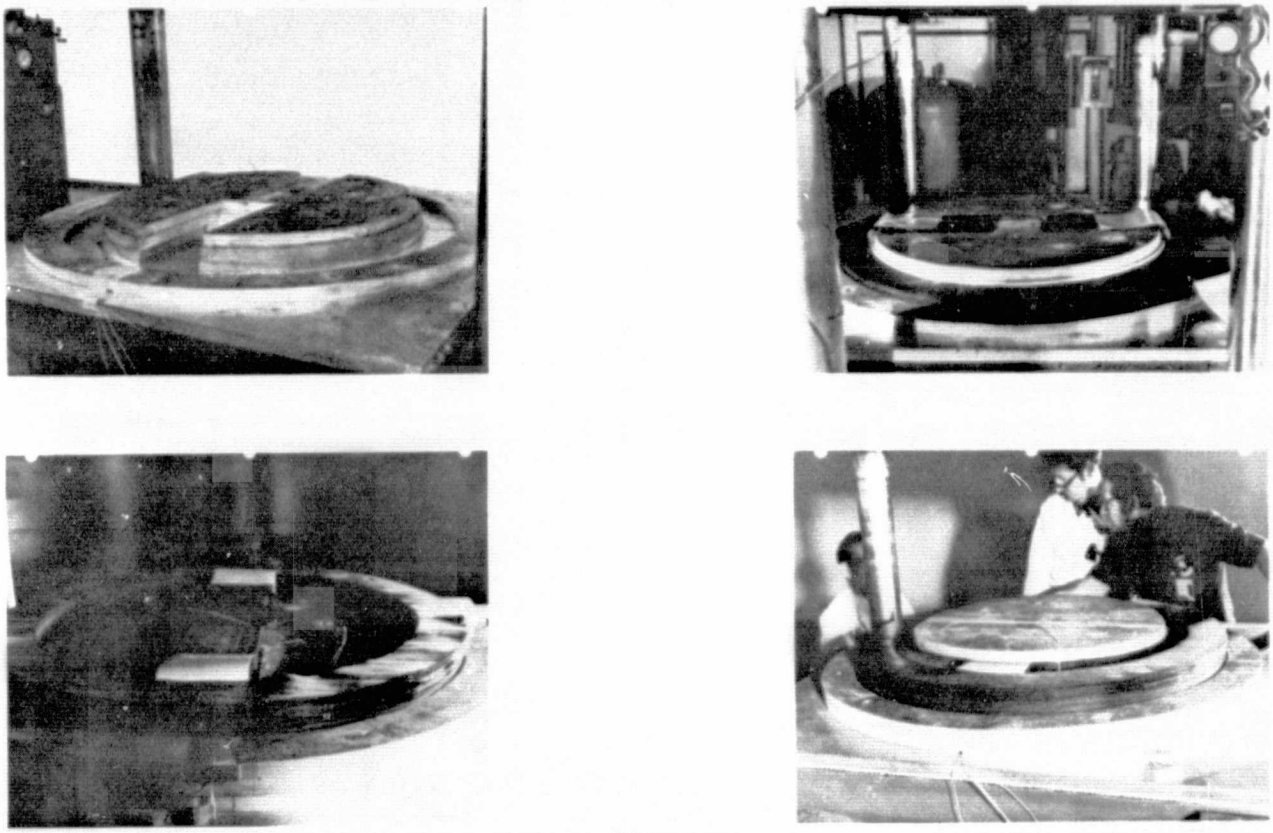

FIGURE 26

FABRICATION SEQUENCE – INITIAL ASSEMBLY OF TOOLING AND PREPREG

L-5 thru L-9 were added in the same manner as ply Set 4 and tooling progressively added as required. The process was continuous and required approximately four hours to assemble the stack.

The top six steps (L-10 thru L-15) that form the nose cap inverse chevron orientation were compressed and assembled in a smaller press using the same procedure and temperature-pressure debulking cycle as used in the bottom steps. The tooling was removed from the small press assembly, the compressed nose cap ply assembly was transferred as a unit to the large press and the tooling was reassembled to complete the heat shield stack (Figure 28). The gaps remaining in the exterior tooling plates indicates the amount of compaction that must occur before the carbon phenolic billet has reached a jell state. The compressible polyurethane foam block spacers shown in Figure 28 were used to retain the exterior tooling plates in place until the large accumulated gap could be reduced within the effective length of the dowel pins. Additional thermocouples were placed during assembly to provide a good temperature mapping of the assembly (Figure 24). Visual observation ports (Figure 28) were located at three different levels through the exterior tooling plates. By removing a wedge shaped block, an observer could visually inspect a 2.5 x 5.0 cm area of the prepreg, determine the resin flow condition and adjust the temperature so as to prevent resin loss during curing.

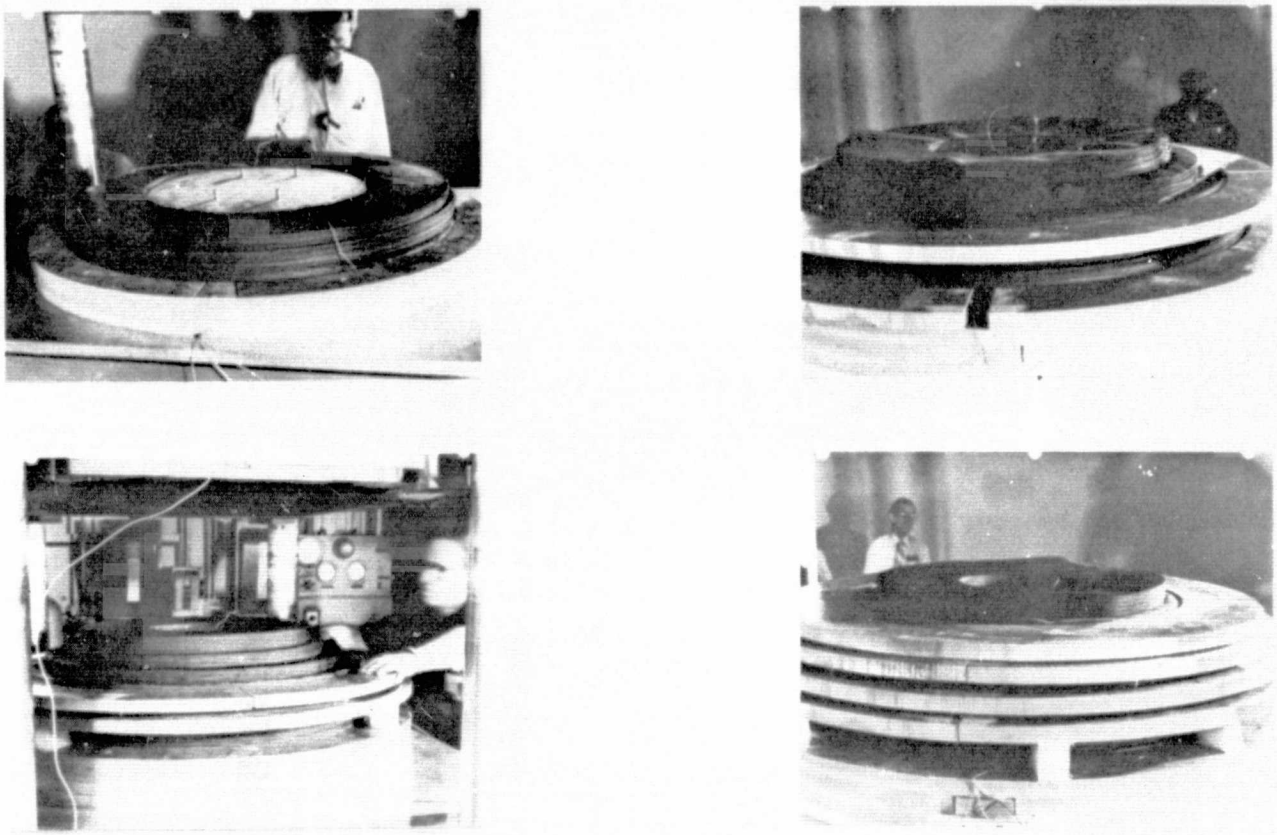

FIGURE 27

FABRICATION SEQUENCE – ASSEMBLY OF STACK MID-SECTION

Cure profile. - Curing of the prepreg into a solid carbon phenolic billet occurred over a 3-day period. Figure 29 presents the cure cycle in terms of temperature, as measured by 8 thermocouples located within the prepreg edges, pressure applied by the press and the remaining accumulated gap thickness. The cure cycle shown in Figure 29 can be subdivided into four phases: (1) assembly of the stack, (2) thermal preconditioning of the prepreg to advance the phenolic resin and prevent resin flow at higher temperature, (3) gradual increase of temperature level of 177°C where polymerization is completed, and (4) slow cool down of the stack.

Assembly of the stack as previously discussed was completed within four hours using compression steps cycles of 34 atm for 10 minutes at 60°C. After the assembly was completed, the temperature was maintained at 60°C for several hours but with very low pressure on the stack. The objective was further advancement of the phenolic resin in order to prevent resin flow at the higher pressures and temperatures. Experience gained during the initial processing development work with small stacks (Section Heat Shield Configuration) had indicated that about four to six additional hours of preconditioning was needed at 60°C prior to increasing the temperature to 177°C. The original curing plan also called for increasing the pressure while the temperature was increased so

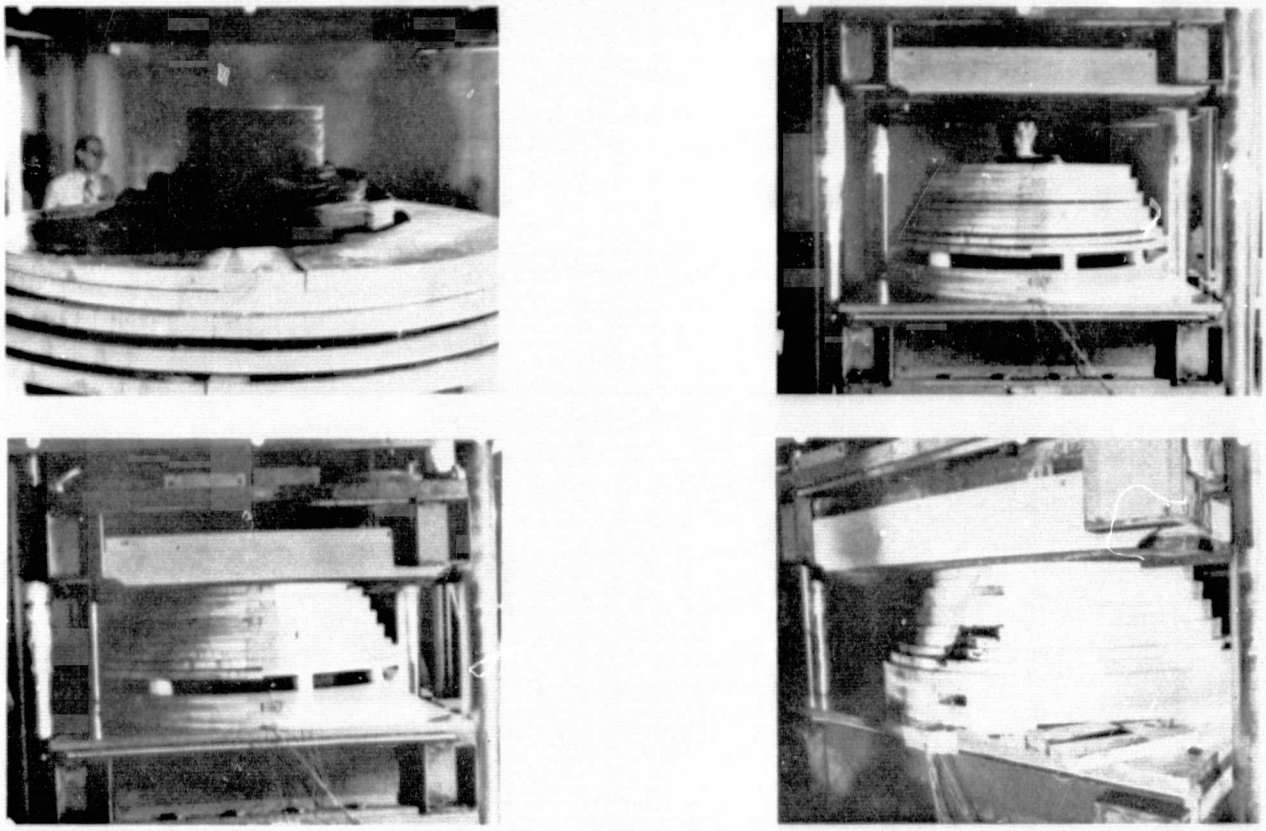

FIGURE 28

FABRICATION SEQUENCE – COMPLETION OF STACK ASSEMBLING AND CURING

that the maximum pressure would be reached just prior to jelling (solidification) of the resin, predicted to occur in the 100°C temperature level. However, in attempting to implement the preconceived curing profile on the full scale stack, excessive resin flow was observed in the 77°C temperature range. The stack temperature was reduced back to the 60°C level and the stack pressure was removed. Cooling of the large stack was slow and some resin was lost, especially in the conical midsection region. (Examination of the thermocouple traces during the preconditioning period indicated that the temperatures lagged in the conical midsection area because of the poor conduction path and the large distance from the heated platens involved. As a consequence, the prepreg in this area was not preconditioned as far as the rest of the heat shield.) Infrared heat lamps were added to increase heating of the midsection area and an asbestos blanket was draped around the perimeter of the press to reduce heat losses and thus minimize internal temperature gradients. A second attempt was made at increasing the temperature and pressure and again excessive resin flow was observed necessitating a return to the preconditioning level. Finally, after almost 30 hours of preconditioning the third attempt in increasing the temperature and pressure was successful and no additional loss of resin was evident. However, the earlier loss of resin and the possibility of not having sufficient plies in each step, resulted in the tooling bottoming-out (all tooling gaps were closed, Figure 28) prior to resin jell. This was an undesirable situation in

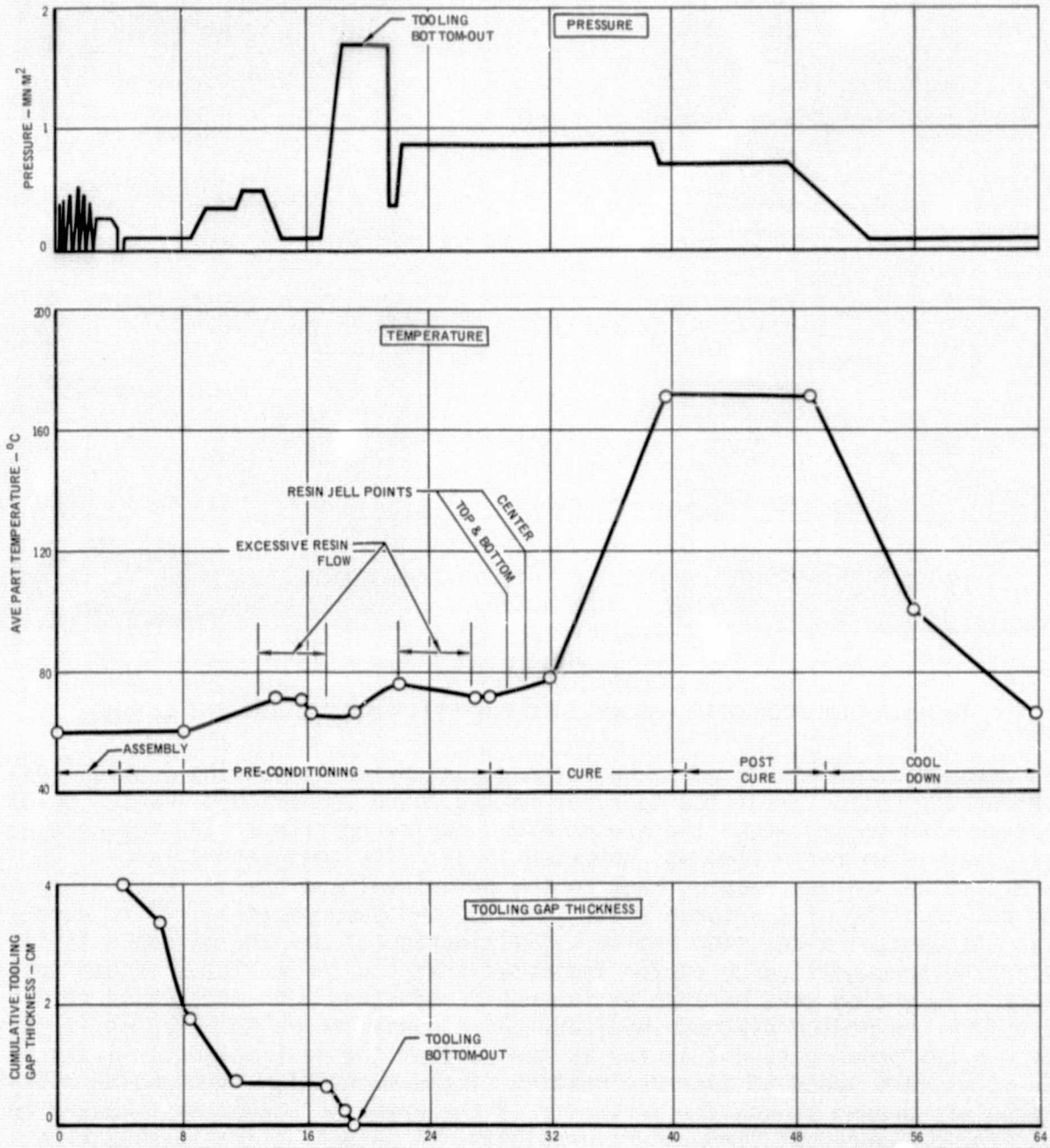

FIGURE 29
MULTISTEP CURING PROFILE

that the pressure was reacted by the tooling rather than by the prepreg plies. In addition, due to the long preconditioning period, the prepreg jelled at a lower temperature than anticipated. As indicated in Figure 29, the temperature of the stack was very gradually increased to 177°C and held at that level for several hours for post-curing. The pressure shown in the figure during this interim was acting on the tooling not on the prepreg. The pressure on the prepreg was undeterminable.

The last phase of the cure cycle involved a very gradual cooling of the entire mass through normal losses to the room temperature environment.

Disassembly of tooling. - When the part and tooling has cooled to 52°C, the press was opened and the exterior tooling was removed (Figure 30). Each tooling ring was in two halves, were pinned to adjacent tooling and all tooling surfaces adjacent to the heat shield billet had a one-eighth inch draft angle on the one inch plate. The gap between the tooling and billet was almost completely filled with excess resin that had solidified. The plates and alignment pins were progressively removed down to the first ring on the bottom, which was bolted to the base plate. The heat shield billet with the internal tooling was then removed from the press as a unit and inverted to permit removal of the interior tooling plates and the two control specimens (Figure 30).

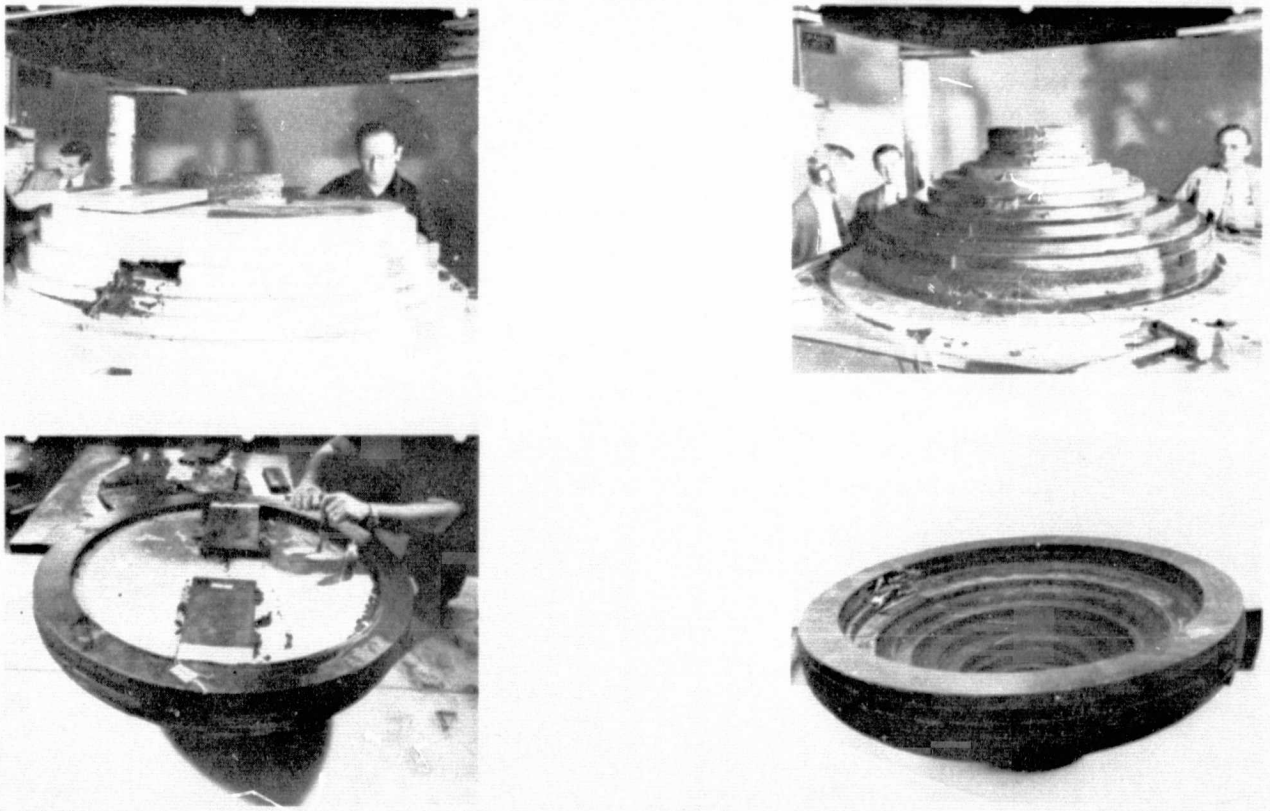

FIGURE 30

FABRICATION SEQUENCE – TOOLING DISASSEMBLY

The first three interior plates containing the process control specimens were removed as a unit, and the two control specimens were then removed from the plates. The interior tooling plates had a one-eighth inch draft to facilitate their removal. The remaining interior tooling plates were removed by inserting threaded rods in the tooling pin alignment holes and prying the plates loose. The finished heat shield billet (Figure 30) at this point weighed 117 Kg. Visual inspection and tapping indicated a solid billet was formed.

Machining of heat shield. - The heat shield billet was placed on a vertical lathe turn table and approximately 3.8 cm of excess material from both sides of the heat shield was rough machined using a single point tungsten carbide cutter (Figure 31). The heat shield was secured to the table in the inverted position through a bolt hole drilled at the nose cap apex where eventually the mass spectrometer inlet tube penetrates the heat shield. During the rough machining operation, delaminations were noticed, especially in the midsection area. Since the single point tool imposes an intense concentrated force on the plies, the delaminated area were impregnated with an epoxy resin to prevent further damage on the heat shield. Epoxy resin was chosen because it cures at room temperature. Finish machining of the heat shield was also accomplished with a single point tool but with a diamond point cutter. Diamonds retain a sharper edge than tungsten carbide and provide a smoother surface finish. Initial errors made in machining the two heat shield penetration holes were corrected by (1) enlarging the nose cap hole to accommodate the larger Jupiter mission penetration assembly, and (2) plugging the initial temperature sensor hole (near the base corner) which did not align with the sensor location on the engineering model, and drilling a new hole at a different circumferential location. The heat shield was mated to the engineering model and some of the mismatches, principally due to the engineering model structure, were reduced by machining local areas of the heat shield inner moldline. In general, the fabrication effort was judged very successful and the feasibility of building a large carbon phenolic mass by the multistep process was demonstrated.

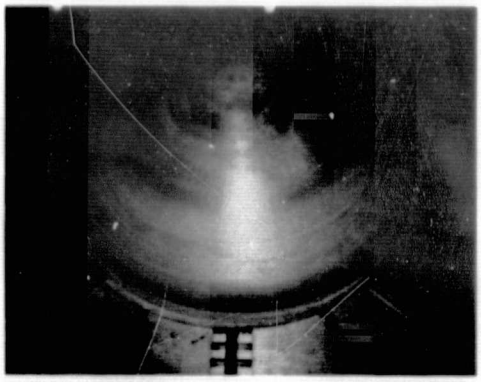

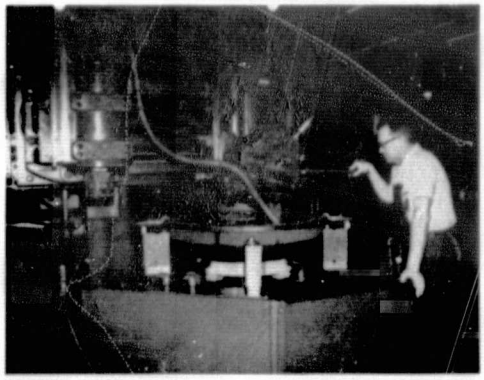

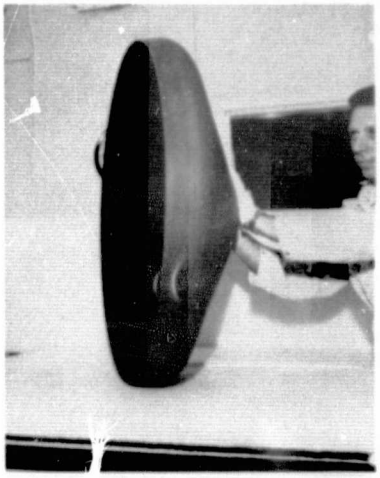

FIGURE 31

FABRICATION SEQUENCE – MACHINING OF HEAT SHIELD

HEAT SHIELD CHARACTERIZATION PROGRAM

The characterization test program had as an objective the determination and evaluation of the integrity and quality of the heat shield made by a new fabrication method. The tests were categorized into two groups: (1) the nondestructive tests performed on the full scale heat shield, and (2) tests made with carbon phenolic specimen that could be tested to destruction to obtain thermal and mechanical property data. Besides basic data acquisition, a secondary objective of the test program was to provide an assessment of the validity of the test approach as a means of characterizing the heat shield material.

Full scale heat shield tests. - The tests performed on the full scale heat shield were intended to assess the quality of the final product without damaging the material. These tests were confined to:

- o Visual Inspection
- o Density Measurement
- o Resin Content
- o X-Ray
- o Ultrasonic

Visual inspection - The heat shield was continuously under observation during fabrication, rough machining and final machining. As discussed in the section entitled, Preliminary Processing Work, some resin loss was observed during fabrication, especially in the conical midsection. During the rough machining operation, very thin delaminations and porous areas became visible which increased in size as the excess material was removed. Most of the delaminations were concentrated in the midsection area but a few were found in other parts of the heat shield. The delaminations could be clearly seen by wiping the surface with MEK solution (the solution fills the gap and presents a darker outline of the crack). A few of the very bad delaminations were sufficiently wide to permit passage of an .04 cm feeler gage through the heat shield. In the areas where delminations occurred, the surface had a porous texture appearance - an indication of resin depletion.

Visual inspection techniques, which can be enhanced with microscopic instruments, are limited to inspection of the external surfaces only. Tapping with a coin, or similar object, can identify large voids beneath the surface but this procedure is a form of ultrasonic testing that was done much more accurately as will be discussed subsequently. At the two locations where the instrument deployment holes were drilled on the heat shield (nose cap and near the base corner, see Figure 21), an opportunity was presented to examine a cross-section of the heat shield. Inspection of the cored plugs and of the holes in the heat shield confirmed the previous assessment that the material in the nose cap was of a better quality than the material in the conical region.

The two plugs cored from the heat shield were examined under high mangification with a Scanning Electronic Microscope (SEM). Photomicrographs of the two core specimen confirmed the presence of cracks that were previously observed visually. Figure 32 shows the crack microstructure for the nose cap plug

magnified 60 to 300 times. Similarly, the photomicrographs of the base corner plug shown in Figure 33 illustrate the lower quality of the heat shield in that area. In examining the photomicrographs, one should bear in mind the high magnification involved and that a machining operation (coring) was performed which may have contributed or even caused the rough surface condition shown in the photomicrographs.

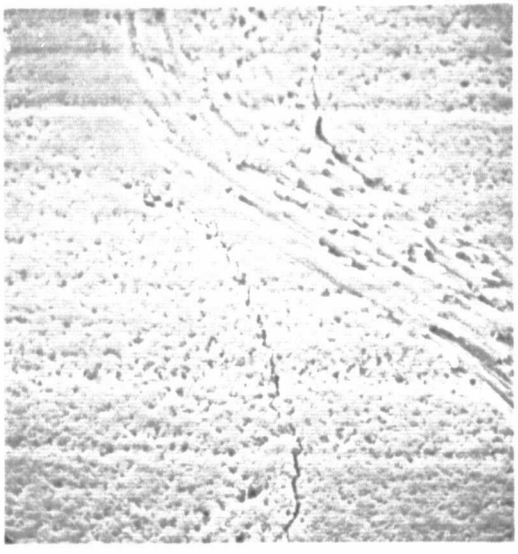

180X

60X

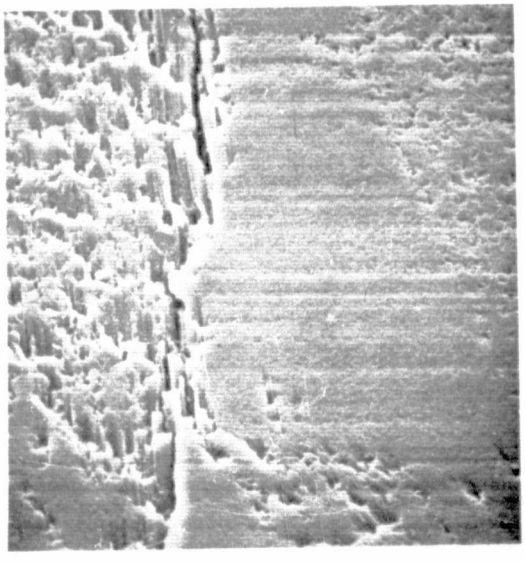

240X

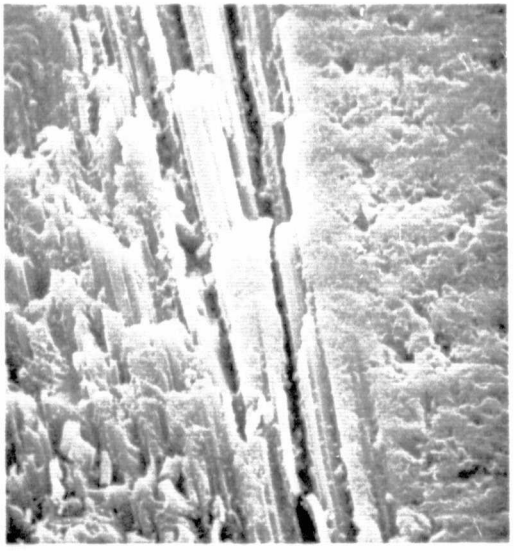

600X

FIGURE 32

PHOTOMICROGRAPH OF NOSE CAP PLUG CORE

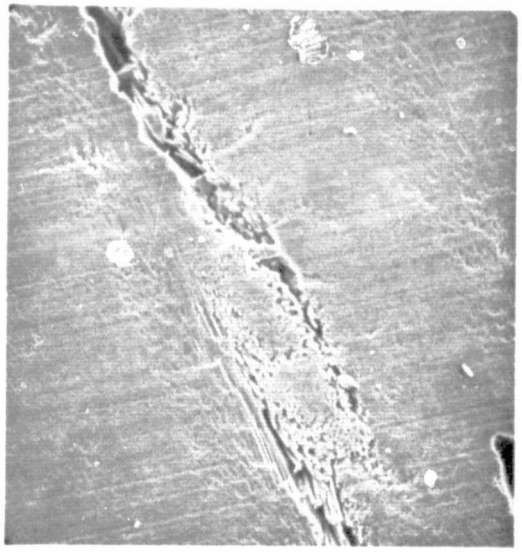

60X

300X

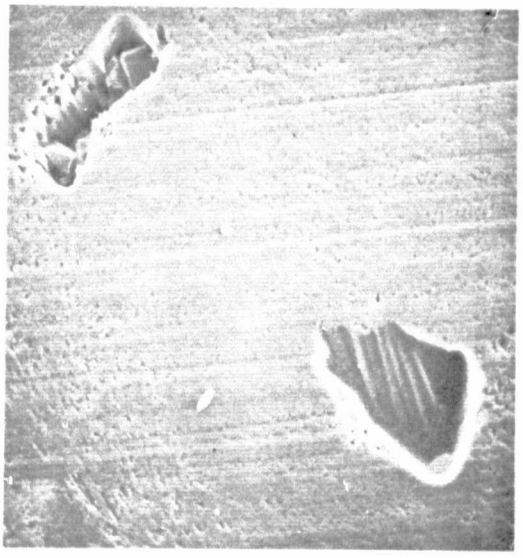

120X

300X

FIGURE 33
PHOTOMICROGRAPH OF BASE CORNER PLUG CORE

The delaminations identified by visual and microscopic means were all between adjacent plies rather than across plies which would have occurred if the carbon reinforcement was sheared. This is very important since the former type presents a much lower risk for the flight heat shield than the latter.

Density measurement - A heat shield density of 1.416 gm/cm^3 was determined by ratioing the measured weight (33.756 Kg) with the heat shield volume computed from the engineering drawing geometry. This density was less than the

densities (1.48) obtained with the carbon phenolic blocks that were not pressed to stops (Section entitled, Prepreg Selection) and is below the target density of 1.45 recommended by Fiberite. The loss of resin and the lack of sufficient pressure on the part due to premature tooling bottoming-out (section entitled, Full Scale FAbrication) were two factors that contributed to the lower heat shield density.

Resin content - Resin content measurements were made on material obtained from the two plugs cored from the heat shield. A standard resin content procedure was used which consisted of grinding the carbon phenolic into a coarse powder, leaching-out the phenolic with an acid solution and weighing the carbon residue. The nose cap plug had a resin content of 33.4% while the base corner plug had a resin content of only 27.6%. The difference in resin content (5.8%) is an indication of the resin lost during curing.

X-rays - X-ray photography is a standard nondestructive test method used to detect cracks and/or internal voids. The x-ray parameters and the different sector layouts are presented in Figure 34. X-ray photographs of the heat shield were taken in two directions: (1) normal to the surface (30° inclination to the plies) for the entire heat shield and (2) parallel to the plies (base corner edge and one sector of the main body to demonstrate the differences from the normal direction). Ply delaminations (cracks) were detected and they appeared as dark lines in the x-rays (see Figure 34A for typical example) when viewed in the parallel direction and as dark zones (Figures 34B and 34C, i.e., the projection of 30° unbonded plies) when viewed normal to the surface. The base corner was also x-rayed parallel to the plies and only sector U-3A revealed two low density areas both approximately 0.148 cm x 1.38 cm. All other edge views were acceptable. It was determined that cracks or delaminations between carbon phenolic plies can be detected and that the x-rays be taken parallel to the ply surfaces. X-rays are useful for this heat shield configuration and thickness (approximate 2.9 cm) for detecting both porous areas and delaminations or cracks.

Ultrasonic - Ultrasonic testing of the full scale heat shield was accomplished by using the test apparatus shown in Figure 35. This test setup provided for data read out on flat charts instead of a preferred polar plot. For a production heat shield, an automated turn table could be utilized and a direct plot of the data could be realized for the design configuration.

The test setup employed by the McDonnell Douglas Quality Assurance Non-Destructive Test Department consisted of an RF transmitter that provided an ultrasonic signal at a frequency of 5.0 MHz and with a power level of 60 db, and a receiver. Two water jets, emanating from the transmitter and receiver and impinging on the heat shield, served as signal carriers and completed the RF circuit (see Figure 35). The test operation was completely automated and ultrasonic signal through the material indicated the degree of heat shield continuity. The sensitivity of the system was adjusted so that unbonded plies would completely attenuate the signal resulting as blank spaces on the chart. These plots or sectors identified as V1 thru V8 are identical to the x-ray views presented in Figures 34A and 34B.

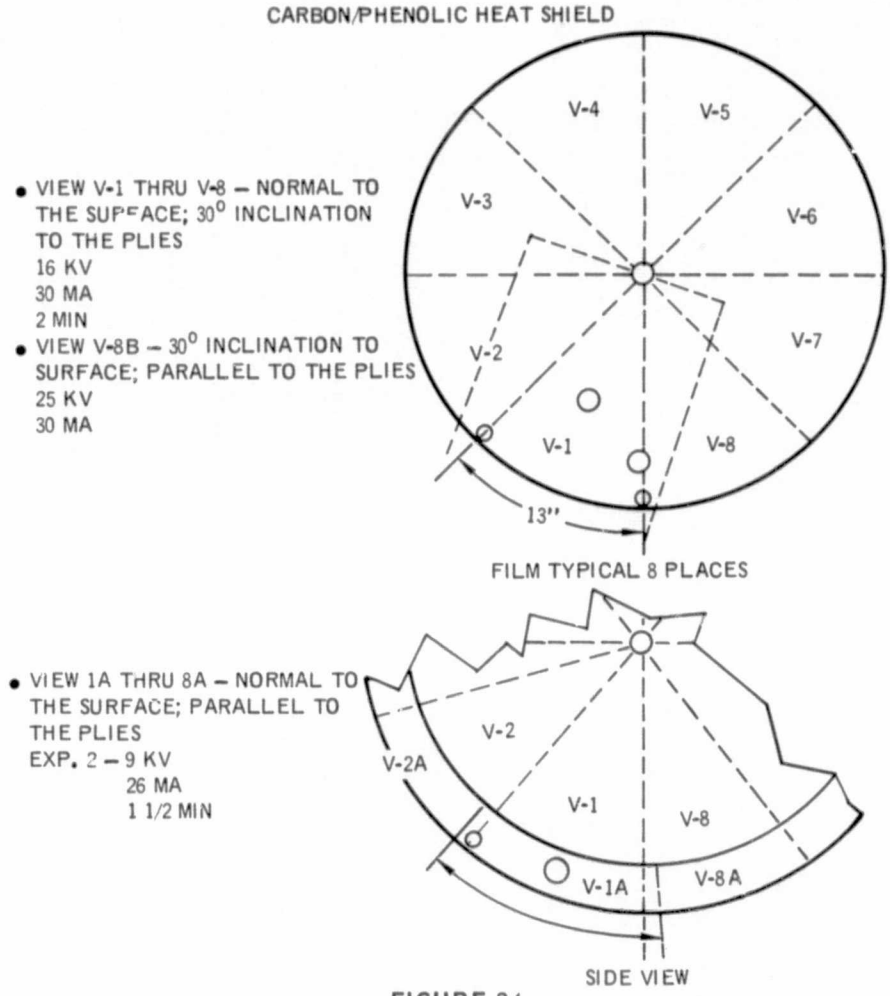

FIGURE 34
X-RAY VIEWS

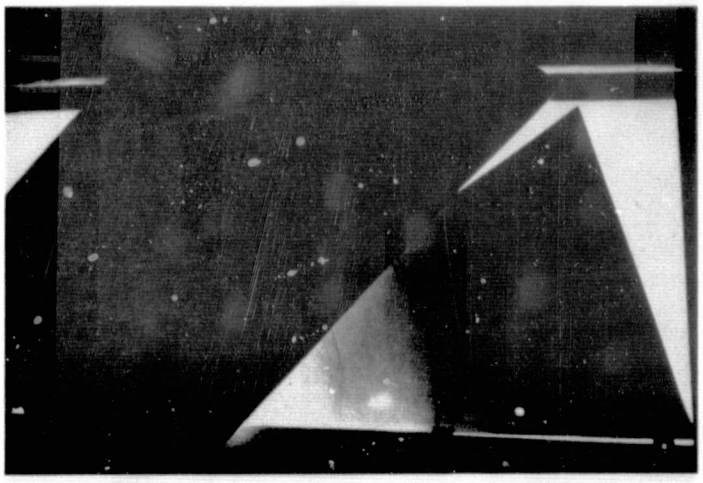

V-8B

NOTES: 1. X-RAY PARALLEL TO THE PLY ORIENTATION
2. DELAMINATIONS APPEAR AS DARK LINES.

FIGURE 34A
X-RAY PHOTOGRAPHS OF SECTOR V-8B

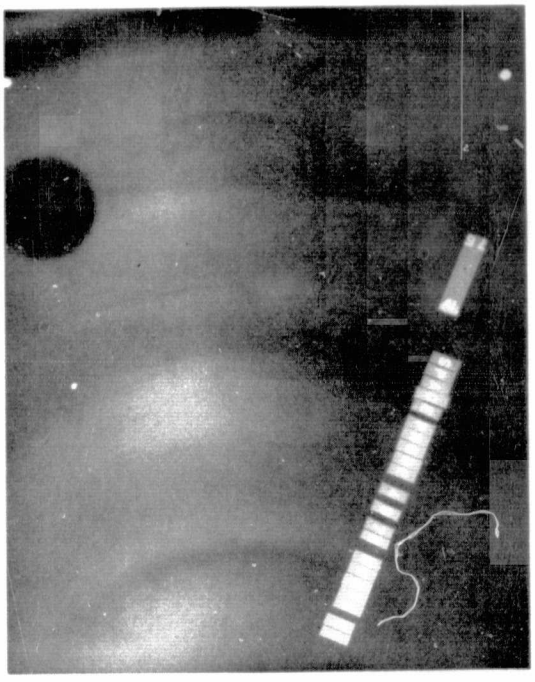

V-1

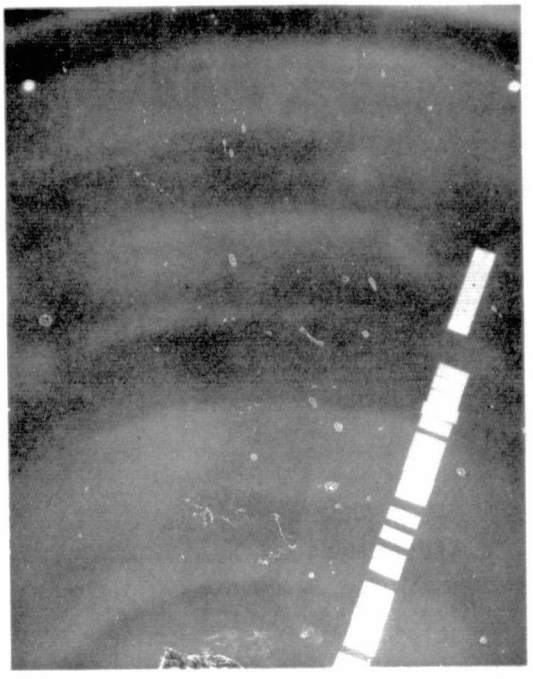

V-2

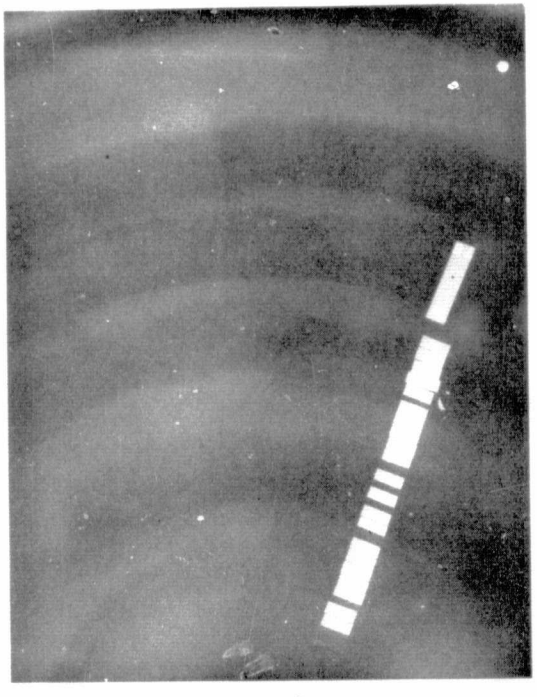

V-3

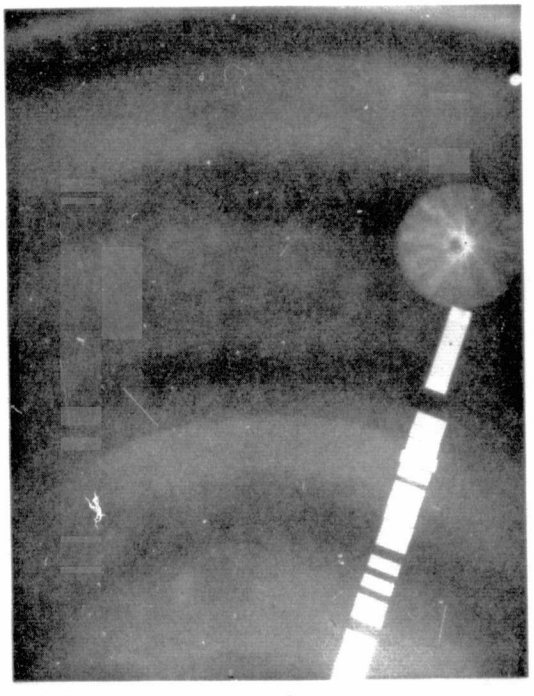

V-4

NOTES: 1. X-RAY NORMAL TO HEAT SHIELD SURFACE – SECTOR V-1 THRU V-4 OF 8 SECTORS
2. DARK AREAS DENOTES LOWER DENSITY (POROSITY AND/OR DELAMINATION)

FIGURE 34B
X-RAY PHOTOGRAPHS – SECTORS V-1 TO V-4

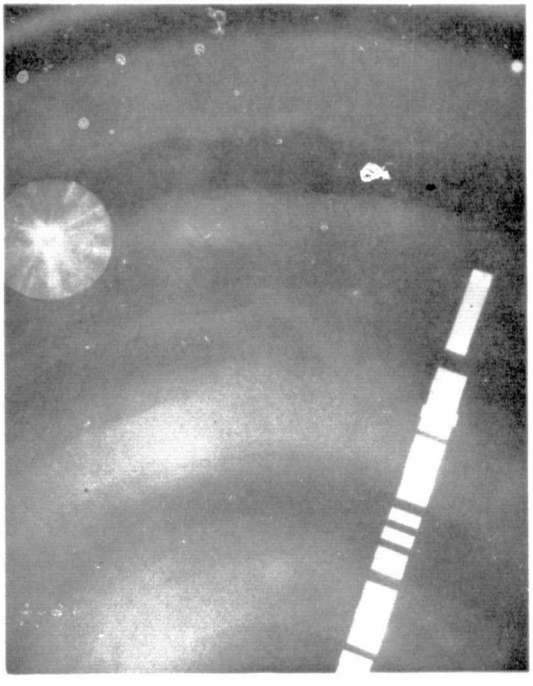

V-5

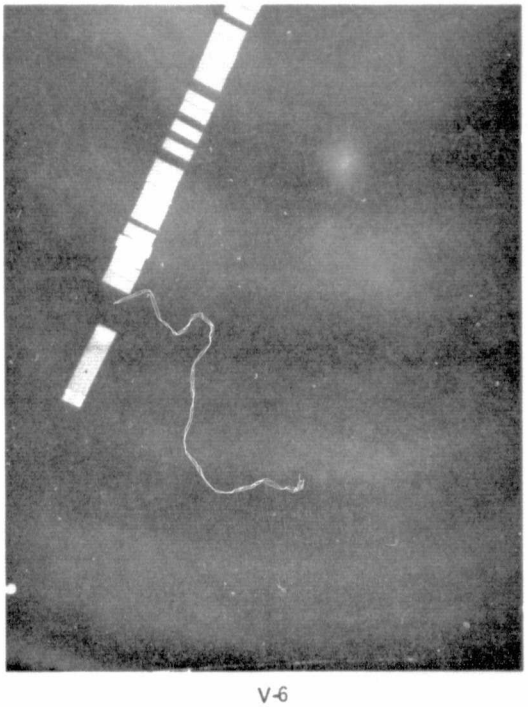

V-6

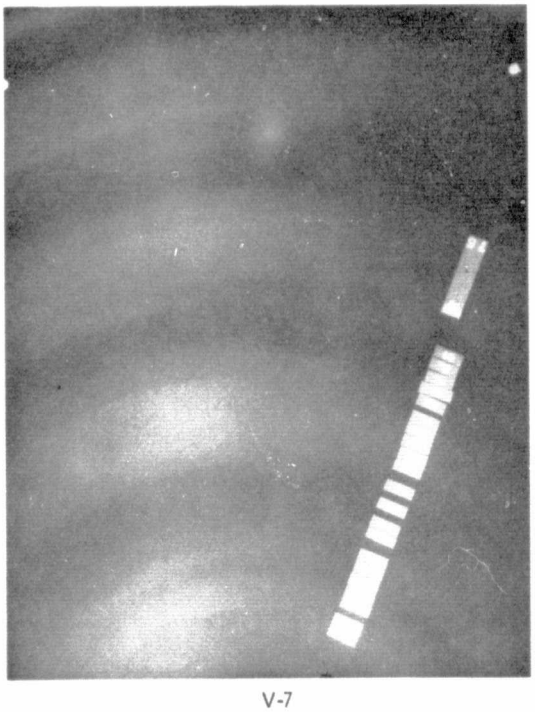

V-7

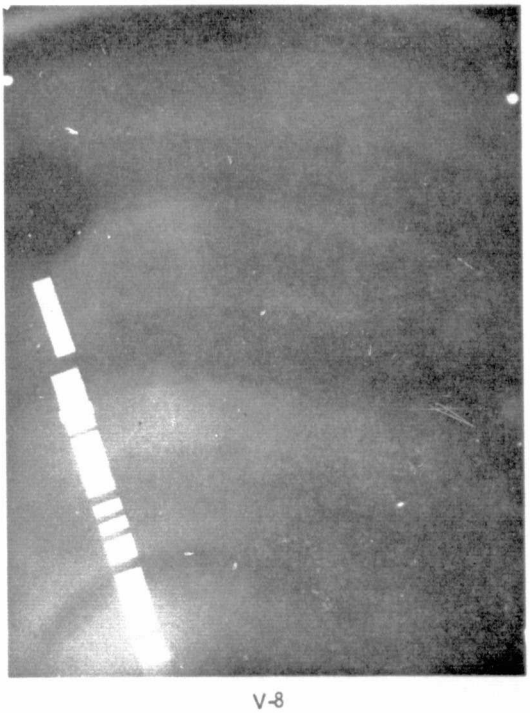

V-8

NOTES: 1. X-RAY NORMAL TO HEAT SHIELD SURFACE – SECTOR V-5 THRU V-8 OF 8 SECTORS
2. DARK AREAS DENOTES LOWER DENSITY (POROSITY AND/OR DELAMINATION)

FIGURE 34C

X-RAY PHOTOGRAPHS – SECTORS V-5 TO V-8

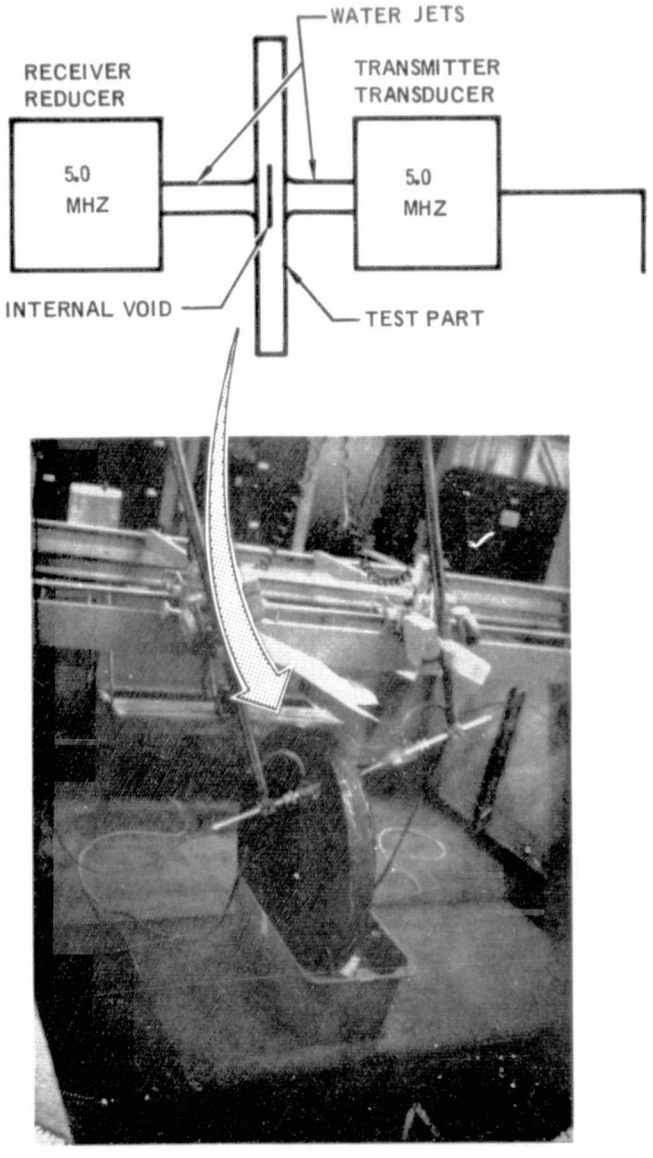

FIGURE 35
ULTRASONIC TEST APPARATUS

The water jet signal carrier was directed normal to the heat shield surface resulting in a 30° ply elevation with respect to the signal. Thus, as shown in Figures 35A and 35B, unbonded plies were seen as zones rather than sharp cracks. Directing the signal parallel to the plies (30° inclination to the surface) leads to signal reflection problems and was not attempted. The light areas in Figures 35A and 35B indicate the presence of porosity or unbonded plies that resulted in a total loss of signal power (60 db). The dark areas had a signal loss of only 20 db and represented a higher density zone.

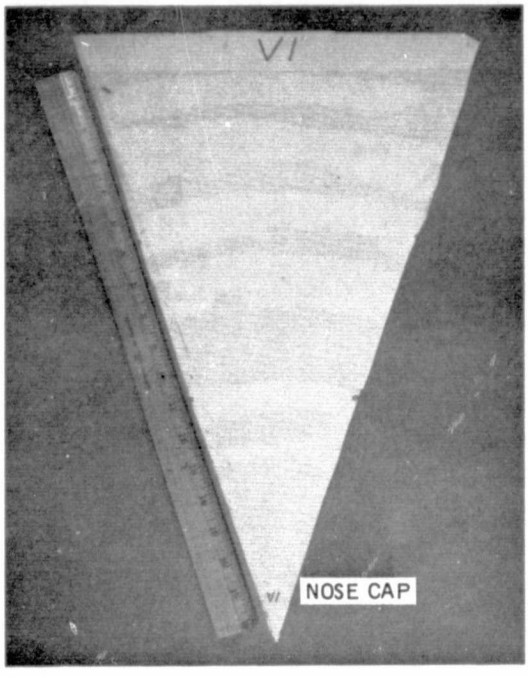

V-1

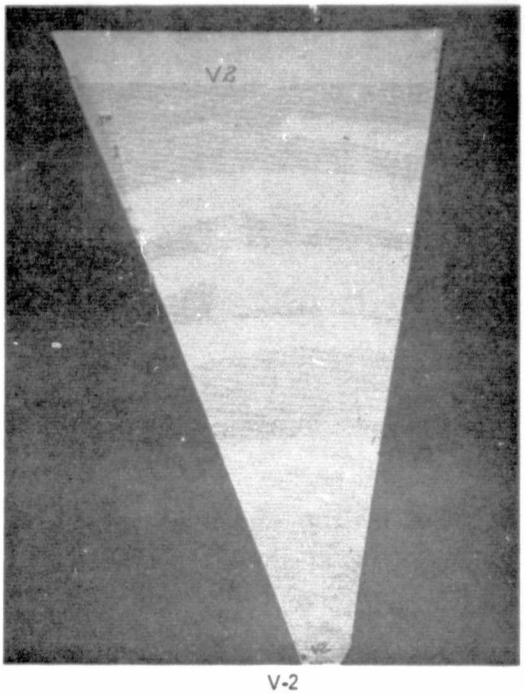

V-2

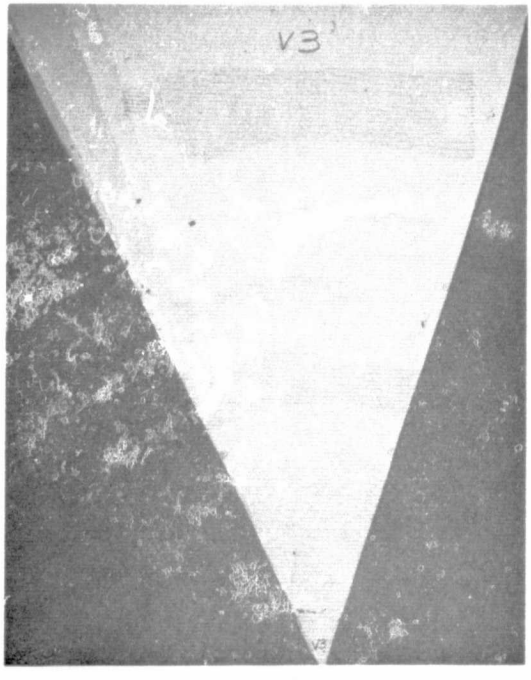

V-3

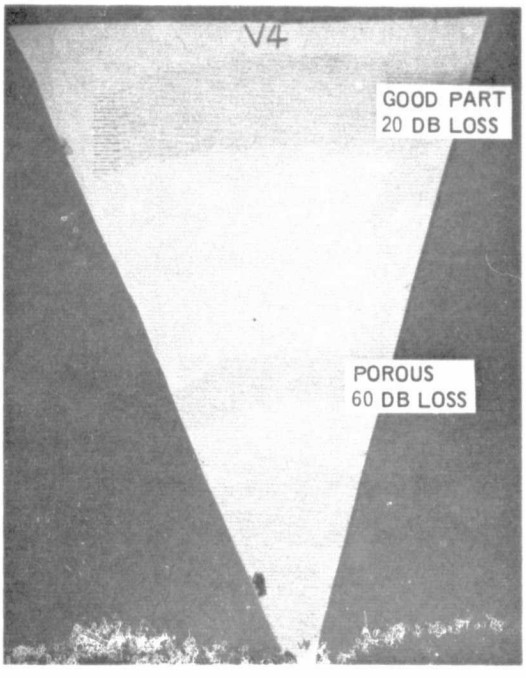

V-4

NOTES:
1. LIGHT AREAS DENOTE DECIBEL LOSSES OF 60 dB's OR GREATER
2. BASIC ATTENUATION IN DARK AREAS IS APPROXIMATELY 34 TO 37 dB's
3. SECTORS V-1 THRU V-4 OF 8 SECTORS

FIGURE 35A

ULTRASONIC MAPPING OF THE HEAT SHIELD
(SECTORS V-1 THRU V-4)

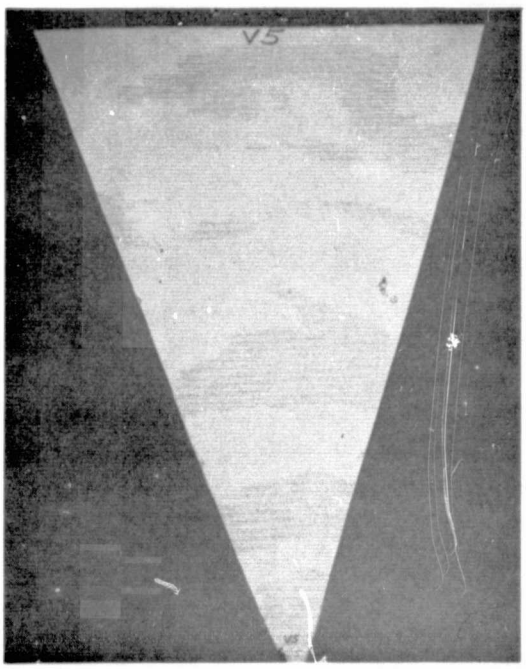

V-5

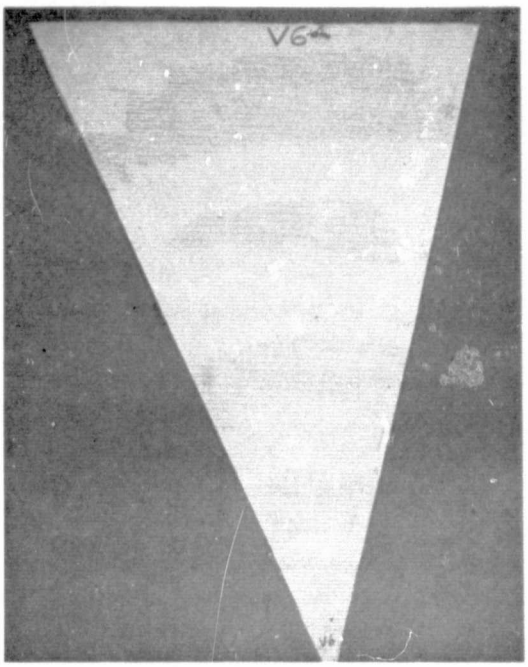

V-6

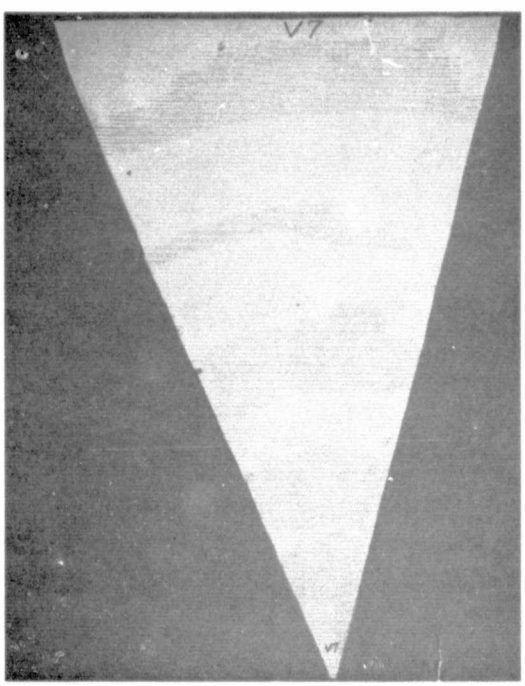

V-7

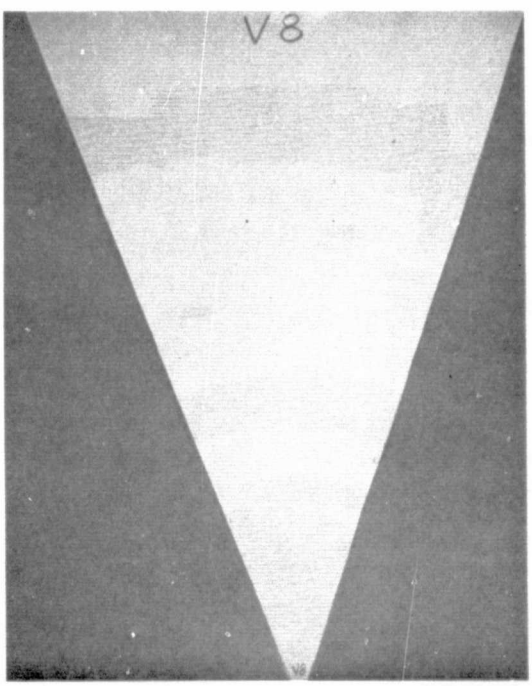

V-8

NOTES:

1. SECTORS V-5 THRU V-8 OF 8 SECTORS
2. LIGHT AREAS DENOTE DECIBEL LOSSES OF 60 dB's OR GREATER
3. BASIC ATTENUATION IN DARK AREAS IS APPROXIMATELY 34 TO 37 dB's

FIGURE 35B

ULTRASONIC MAPPING OF THE HEAT SHIELD
(SECTORS V-5 THRU V.8)

Specimen tests. - Thermal and mechanical property tests were conducted using specimen material that was processed along with the full scale heat shield. Included in these tests were:

- o Flexure
- o Cross laminar tensile
- o Interlaminar shear
- o Plasma arc (specimen provided for testing at NASA-ARC).

The data from these tests were used to quantitatively assess the quality of the full scale heat shield.

The representative heat shield specimen were cut from the carbon phenolic blocks built along and within the heat shield tooling (Figure 21). Delaminations were also evident within these blocks and care was taken to select the better portion of the block for specimen material. The specimen that served as standards for comparison were obtained from previously built billets from which the missile flight heat shields were cut from. These billets were made with MXC-31 prepreg material. A few specimens were also cut from Blocks 8 and 9 (section entitled, Prepreg Selection) that were made during the preliminary processing work phase.

Flexure tests - Tests were conducted to determine the in plane flexural strength and stiffness of the heat shield material.

Specimens were flexural bars 12.7 cm long by 1.27 cm wide and 0.5 cm thick. The cloth was oriented parallel to the length and width of the specimens.

The flexural test setup is shown schematically in Figure 36. The specimens were loaded by a four point load fixture and midspan deflection was measured as a function of applied load. All tests were conducted at room temperature in air in a 9,000 Kgm Ballwin testing machine.

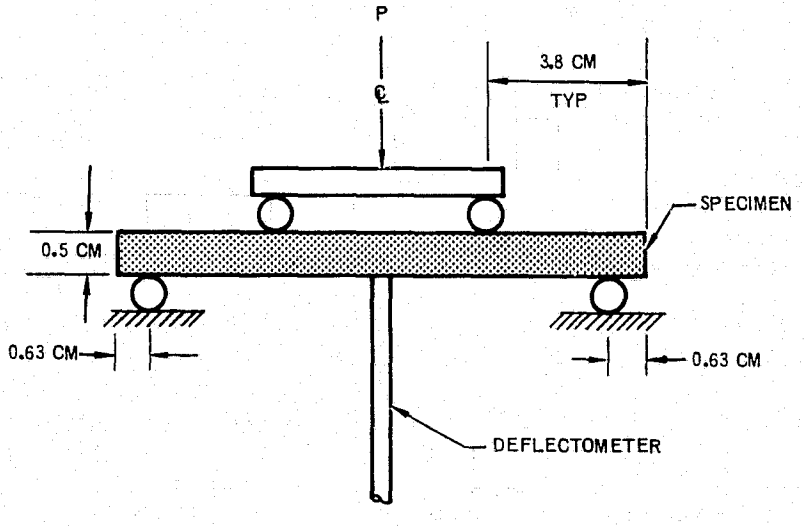

FIGURE 36

FLEXURE TEST SETUP

A total of six specimens from control specimen #1 were tested and test results are presented in Figure 37. Average flexural strength is 172 MN/m^2 which is about 96% of published minimum values and average flexural modulus is 21900 MN/m^2 which is about 17% higher than published values.

MATERIAL BLOCK	SPECIMEN NO.	F_{FLEX} (MN/m^2)	E_{FLEX} (MN/m^2)
1	1	187	22,600
1	2	181	23,100
1	3	170	19,600
1	4	156	20,900
1	5	163	22,300
1	6	175	23,200
	AVERAGE	172	21,900

FIGURE 37
FLEXURE TEST RESULTS

Flexural test results indicate that the heat shield material flexural strength is slightly less than is normally considered as acceptable while the flexural modulus is higher than expected. The measured flexural test results indicate that a structurally adequate heat shield could be fabricated.

Cross laminar tensile tests - Tests were conducted to determine the cross laminar tensile strength of the heat shield material.

Specimens were solid circular cylinders of 6.45 cm^2 area. The ply orientation was perpendicular to the length of the cylinders.

The cross laminar tensile test setup is shown schematically in Figure 38. The specimens were bonded with FM 123 adhesive to cylindrical loading blocks. The loading blocks were axially loaded and failure load was recorded. All tests were conducted at room temperature in air in a 9,000 Kgm Ballwin testing machine.

A total of 17 specimens were tested, 3 from material block 9, 3 from the excess heat shield nose cap material, 3 from material block 1 and 7 from material block 1 after reimpregnation with epoxy resin. Test results are given in Figure 39.

Specimens from material block 9 had an average strength of 8.4 MN/m^2. Specimens from the nose cap material had an average strength of 6.2 MN/m^2. Specimen from control specimen #1 had an average strength of 6.1 MN/m^2. Specimens from material block 1 after reimpregnation had an average strength of 6.2 MN/m^2. As noted in Figure 39 several specimens failed at the FM123. Specimen interface and these test values were not included in the strength averages.

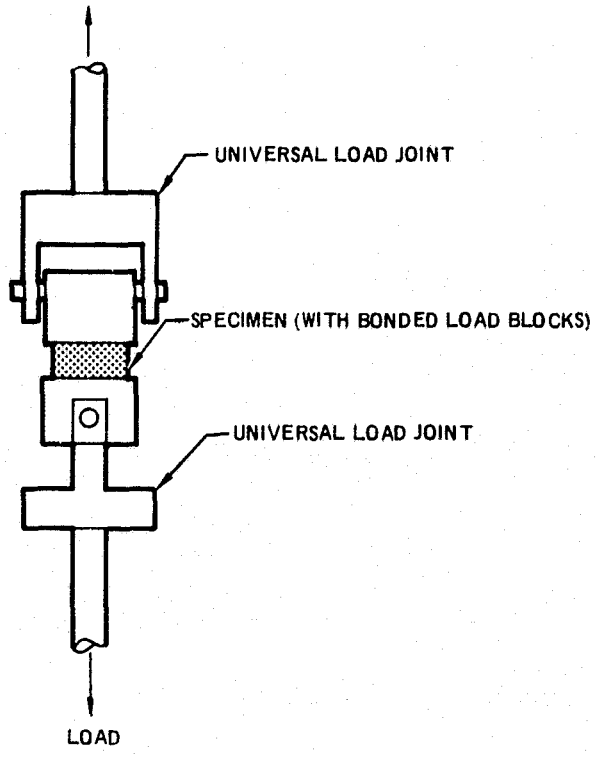

FIGURE 38

CROSS LAMINAR TENSION TEST SETUP

MATERIAL BLOCK	SPECIMEN NO.	F_{TU} (MN/m^2)	AVERAGE F_{TU} (MN/m^2)
9	1	6.0**	
9	2	8.2	8.4
9	3	8.6	
NC	1	3.4	
NC	2	8.2	6.2
NC	3	7.1	
1	1	6.8	
1	2	5.1	6.1
1	3	6.4	
1	R1	4.0	
1	R2	2.7	
1	R3	5.5 **	
1	R4	1.2	
1	R5 *	5.4	
1	R6	3.5	
1	R7	6.7	6.2
1	R8	8.6	

*REIMPREGNATED

**FAILURE AT FM123 – SPECIMEN INTERFACE

FIGURE 39

CROSS LAMINAR TENSILE TEST RESULTS

Cross laminar tensile strength test results indicate that the heat shield material cross laminar tensile strength is lower than normally considered as acceptable. In addition, the quicky-type reimpregnation did not significantly improve the strength. Scatter of test data may also indicate that cross laminar tensile strength varies considerably throughout the heat shield, probably due to random ply delaminations.

Comparison of test results with the preliminary estimates of required cross laminar strengths given in Figure 8 indicate that the present heat shield material would not qualify for flight.

Interlaminar shear tests - Tests were conducted to determine the interlaminar shear strength of the heat shield material.

Specimen were 10 cm long bars 1.27 cm wide and 0.5 cm thick. Overlapping notches in the specimens at mid length induced shear failure of the specimens along the laminate bonds. The cloth orientation was parallel to the length and thickness of the specimens.

Interlaminar shear test setup is shown schematically in Figure 40. The specimens were gripped at each end by clamp on universal grips. The specimens were loaded in axial tension and failure load was recorded. All tests were conducted at room temperature in air in a 9,000 Kgm Ballwin testing machine.

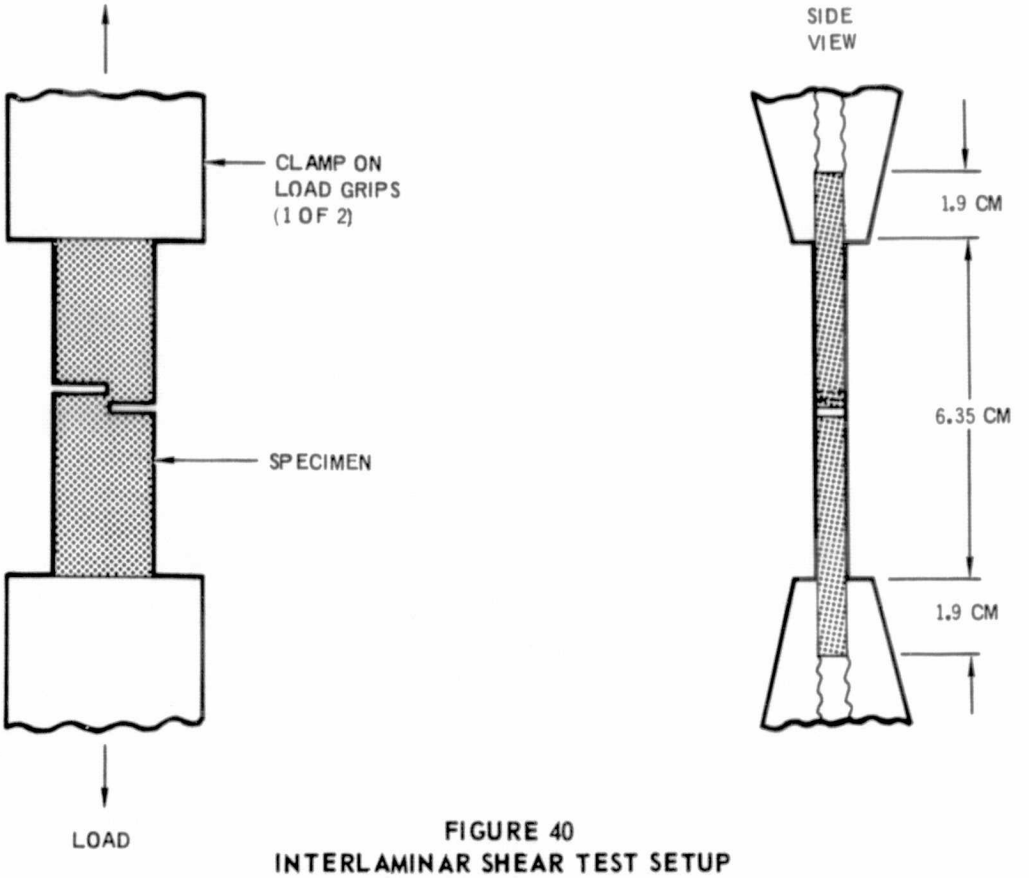

FIGURE 40
INTERLAMINAR SHEAR TEST SETUP

A total of 8 specimens were tested, 4 from material block 8 and 4 from control specimen #1. Test results are given in Figure 41. Specimens from material block 8 had an average strength of 11.2 MN/m^2 and specimen from material block 1 had an average strength of 8.6 MN/m^2.

MATERIAL BLOCK	SPECIMEN NUMBER	F_{SU} (MN/m^2)	AVERAGE F_{SU} (MN/m^2)
8	1	14.1	
8	2	9.8	
8	3	8.5	11.2
8	4	12.4	
1	1	7.2	
1	2	9.8	
1	3	12.4	8.6
1	4	5.2	

FIGURE 41

INTERLAMINAR SHEAR TEST RESULTS

Interlaminar shear strength test results indicate that the heat shield interlaminar shear strength is lower than normally considered acceptable. However, comparison of test results with the preliminary estimates of required shear strengths of the heat shield given in Figure 8 indicate that a structurally adequate heat shield material could be fabricated (with a factor of safety of 1.25.).

Plasma arc tests - Plasma arc testing of specimen representative of the heat shield is a direct method of assessing material performance in an environment that is representative of the intense entry heating condition. Until the Ames Giant Arc Facility becomes operational, current plasma arc facilities cannot match the planetary entry heating levels depicted in Figures 3 through 5. However, they can provide heating rates that are sufficiently high to attain surface temperatures and temperature gradients that are comparable to the flight heat shield values depicted in Figures 6 and 7. Matching of the temperatures is very important in assessing the integrity and strength of a char forming material, such as carbon phenolic.

Plasma arc testing was conducted in the Ames Advance Entry Heating Simulator (AEHS) in early June of 1976. The AEHS Facility, described in Reference 10, provides a combined convective-radiative heating environment, similar to but of much lower magnitude than encountered in planetary entries.

The test program was comparative in nature and was intended to assess the performance of the presently made heat shield material with the previously flight qualified carbon phenolic. Figure 42 identifies the source and dimensions of the eighteen (18) specimen. The test matrix included three groups of specimen obtained from (1) the MXC-31 billet (reference flight heat shield material),(2) the control specimen fabricated with the full scale heat shield (see Figure 21), and (3) block #9 that was molded without stops during the preliminary processing work. The splash model specimen configuration

SPECIMEN NO.	ORIGINAL WEIGHT GRAMS	GRAPHITE O.D. INCHES	CARBON PHENOLIC O.D. INCHES	SPECIMEN LENGTH INCHES
o MXC-31 REFERENCE MATERIAL (COMPRESSION MOLDED @ 1000 PSI WITH VERY LITTLE RESIN FLOW)				
MXC-31-1	27.9373	.826	0.625	1.003
-2	31.4290	.827	0.625	1.003
-3	28.1820	.828	0.625	1.003
-4	28.3025	.827	0.625	1.002
-5	28.1182	.826	0.625	1.005
-6	28.0788	.826	0.625	1.001
o MX 4910 HP FABRICATED ALONG WITH THE FULL SCALE H/S (COMPRESSION MOLDED TO TOOLING STOPS @ 370 PSI EXCESSIVE RESIN FLOW)				
• CONTROL SPECIMENS FROM THE FULL SCALE OPP SRT HEAT SHIELD BLOCKS #1 AND 2				
BLOCK				
CS-1	31.9889	.826	0.625	1.003
-2	28.2770	.826	0.625	1.003
-3	27.9321	.826	0.625	1.003
-4	28.2039	.826	0.625	1.003
#1 2D-1	31.5335	.826	0.625	1.003
#1 2D-2	31.6007	.826	0.625	1.003
o TEST SPECIMEN #9 MX 4910 HP (COMPRESSION MOLDED WITHOUT STOPS @ 370 PSI VERY LITTLE RESIN FLOW)				
9-1	24.3752	.826	0.625	.755
9-2	24.2506	.826	0.625	.755
9-3	24.6472	.826	0.625	.755
9-4	24.4172	.826	0.625	.755
9-5	24.5026	.826	0.625	.755
9-6	24.2811	.826	0.625	.755

FIGURE 42

PLASMA ARC TEST SPECIMEN INITIAL DATA

is illustrated in Figure 43. A graphite sleeve was fitted and bonded over the specimen in order to retain the "free" edges of the specimen plies.

Figure 44 summarizes the test results. All of the specimen were tested at nearly the same test condition: stagnation pressure of .80 atm, radiative flux of 1.6 kw/cm^2, convective heating of 1.4 kw/cm^2 and a test duration of about 6.0 seconds. From a comparison of the recession rate data and visual inspection of each specimen, it was concluded that within the scatter of the data, the carbon phenolic material processed with the multi-step compression method performed as well as the flight qualified material.

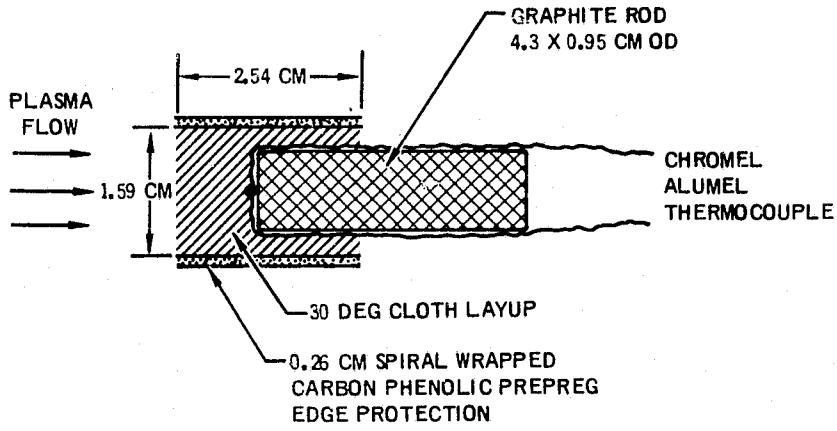

FIGURE 43
PLASMA-ARC SPECIMEN CONFIGURATION

SPECIMEN IDENTIFICATION	TEST CONDITIONS				RESULTS		
	PRESSURE ATM	RADIATIVE FLUX KW/CM^2	CONVECTIVE FLUX KW/CM^2	DURATION SEC	SURFACE TEMP. ^{0}K	TOTAL RECESSION CM	RECESSION RATE CM SEC
MXC-31-1	0.92	1.69	1.43	6.10	3236	0.152	0.025
MXC-31-2	0.61	1.53	1.36	6.4	3491	0.147	0.023
MXC-31-3	0.92	1.69	1.43	5.65	3405	0.160	0.028
MXC-31-4	0.80	1.46	1.37	6.05	3289	0.137	0.023
MXC-31-5	0.79	1.44	1.34	5.72	3306	0.109	0.019
MXC-31-6	0.80	1.46	1.37	5.85	3424	0.127	0.022
AVERAGE	0.81	1.54	1.38	5.9	3358	0.139	0.023
CS-1	0.92	1.69	1.43	5.60	3534	0.058	0.011
CS-2	0.92	1.69	1.43	4.35	3499	0.066	0.015
CS-3	0.80	1.46	1.37	6.10	3381	0.142	0.023
CS-4	0.79	1.44	1.34	6.08	3169	0.096	0.016
NO. 1 2D-1	0.61	1.53	1.36	6.0	3551	0.167	0.028
NO. 1 2D-2	0.78	1.81	1.41	5.85	3634	0.132	0.023
AVERAGE	0.80	1.60	1.39	5.66	3495	0.110	0.019
9-1	0.61	1.53	1.36	5.85	3363	0.122	0.021
9-2	0.83	1.58	1.37	5.72	-	0.038	0.007
9-3	0.78	1.81	1.41	5.9	2770	0.110	0.018
9-4	0.83	1.68	1.37	3.28	-	0.081	0.025
9-5	0.78	1.81	1.41	6.1	3211	0.191	0.031
9-6	0.79	1.44	1.34	5.88	3177	0.137	0.023
AVERAGE	0.77	1.66	1.38	5.45	3130	0.113	0.021

FIGURE 44
PLASMA ARC TEST RESULTS

HEAT SHIELD COST AND SCHEDULE DATA

The cost and schedule data associated with the fabrication and characterization of the SUAEP heat shield were compiled and used to estimate the cost and time involved in fabricating a flight heat shield. This information is considered proprietary for general dissemination in this report but was transmitted to NASA-ARC as a separate addendum.

FABRICATION PROCESSING IMPROVEMENTS

Fabrication of the full scale probe heat shield has demonstrated the feasibility of the multistep concept in molding large carbon phenolic billets. However, in the course of the fabrication activity a number of problems were identified which necessitate improvements in the processing technique in order to achieve a flight heat shield. The problems encountered during fabrication were noted in Section 5.0 and the general areas where improvements are required are listed and discussed below:

(1) Determination of the prepreg "B"-staging level.
(2) Refinement of the pressure-temperature-time-cure cycle.
(3) More uniform pressure application during curing.
(4) More uniform heating during curing.
(5) Use of a rotating cutting tool.
(6) More accurate nondestructive evaluation techniques.

Items (1) and (2) are interrelated in that the cure cycle time history is strongly dependent on the initial "B"-staging level. The prepreg for this program was purposely bought in a less advanced condition and was further advanced in-house first in an oven and later in the press at about 66°C for several hours. The prepreg for the next fabrication activity should be "B"-staged at a higher temperature-time level to retard resin flow and to shorten the fabrication cycle.

Better control of the level and uniformity of pressure and temperature is essential to producing a heat shield without delmainations or unbonded plies. In the present fabrication effort, a very simple and inexpensive tooling was employed. A drawback of the present tooling was that first, it applied an uneven pressure on the stack during the compression and curing cycle with higher pressures imposed on the nose cap (smaller surface area) and less pressure on the larger diameter rings. Second, the tooling transferred pressure to the prepreg until the tooling bottomed-out (i.e., metal-to-metal contact); thereafter, additional pressure could not be transferred to the stack. More uniform pressure application can be achieved by incorporating spring loading on the tooling as conceptually illustrated in Figure 45. This tooling concept requires additional engineering and evaluation prior to commitment. The simple tooling employed in this program may be adequate and the unbonded heat shield plies may have been entirely due to excessive resin loss (insufficient temperature conditioning), use of a relative "green" prepreg and/or not enough plies in each step that resulted in premature bottoming-out of the tooling.

The stack temperature distribution was easier to control, especially after the press was closed. However, a significant temperature lag was evident in the cone midsection area which is the area furthest from the heated press plates. The control specimen blocks (Figure 21) contributed to the poor heat transfer path and may require relocation. Auxiliary heaters properly located and controlled can greatly improve the temperature control of the stack.

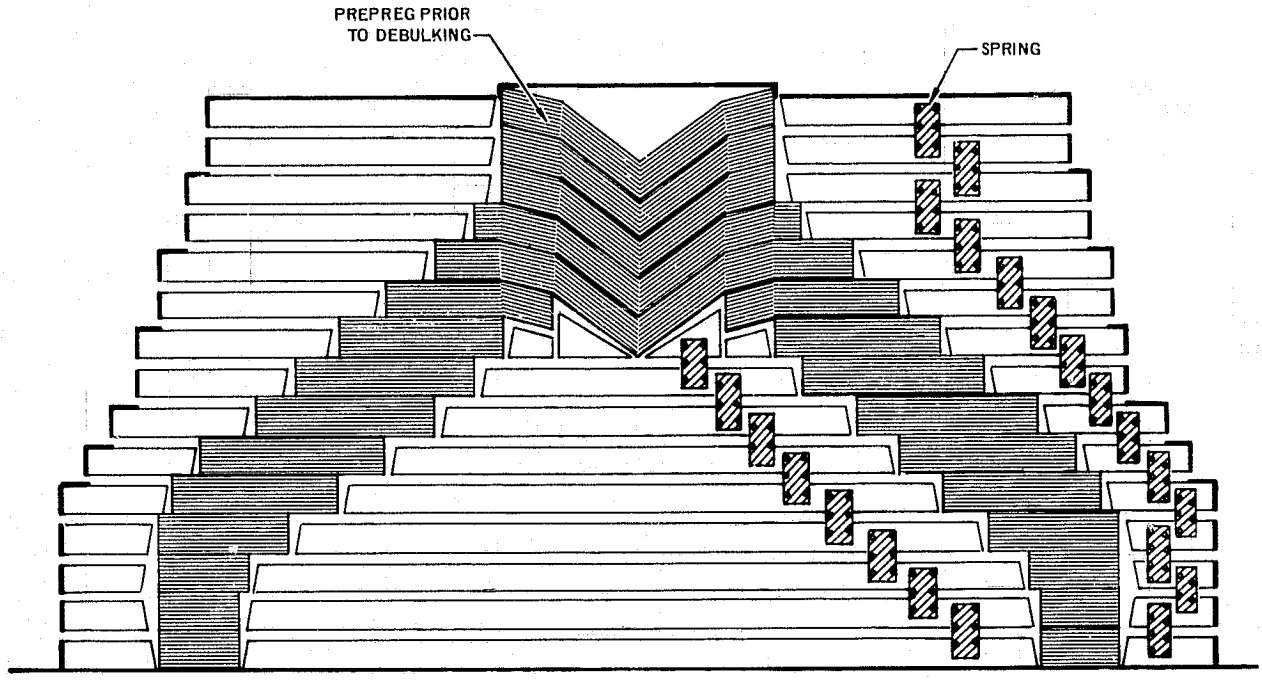

FIGURE 45

SPRING LOADED TOOLING CONCEPT

In the heat shield machining operation, the single-point cutting tool exerted very intense local pressure that may have weakened the interlaminar strength of the plies. A rotating tool that removes material by a grinding/cutting action and avoids the concentrated loading of the single-point tool is recommended for future programs.

The Nondestructive Tests (NDT) performed on the present heat shield included visual inspection with the aid of MEK solvent, x-rays and ultrasonics. These methods can uncover large voids or delaminations but not the very fine imperfections. Neutron particle detection methods have been developed and successfully used in NDT of composite materials and should be used in future probe heat shields.

CONCLUSIONS AND RECOMMENDATIONS

The primary accomplishment of this SR&T activity was the full scale fabrication of the probe carbon phenolic heat shield. The fabrication activity was judged successful and thus, the feasibility of the multistep processing method has been demonstrated as a viable approach in forming billet sizes greater than have ever been molded in the past. Some delaminations or unbonded plies were evident but these will be eliminated by future processing development work based on the experience gained in this program.

In terms of fabrication experience, it was learned that: (1) debulking and assembly of the preprepg and tooling could be accomplished more rapidly than had previously been anticipated; (2) the preconditioning and curing duration was much too long (the prepreg was too "green"); (3) the tooling bottomed-out prematurely thus preventing sufficient pressure loading on the plies (may need more plies per step or a spring-loaded tooling concept); (4) exothermic reactions did not present any temperature control problems during curing (thickness of billet was limited to manageable levels); and (5) forming the cone and the nose cap with the inverse chevron as an integral unit did not add any significant fabrication complexities.

The heat shield characterization tests and preliminary structural analysis indicated that local selected material had adequate mechanical strength. Both the x-ray and especially the ultrasonic tests were able to identify the unbonded plies where mechanical strength was inadequate.

It is recommended that future fabrication work should utilize a prepreg that is further "B"-staged than the material used in this program and that consideration be given to selecting a prepreg without the carbon fillers in order to achieve greater interlaminate strength. Improved tooling concepts that can provide more uniform pressure and temperature on the stack should be evaluated. The most logical next step would be to conduct process development tests and scale up activities with full scale tooling. This recommendation serves to verify the multistep procedure and has the dual purpose of containing the processing work initiated in this program and targeting the heat shield for the first probe mission to the outer planets.

REFERENCES

1. McDonnell Douglas Astronautics Company-East, "Saturn/Uranus Atmospheric Entry Probe, Final Report, Contract NAS 2-7328," Report MDC E0870, 11 July 1973.

2. Mitchell, G. D., et.al., "Development Support of a Full Scale Saturn/ Uranus Engineering Model," NASA CR-137726, January 1976.

3. "Outer Planet Atmospheric Entry Probe - System Description," presented at the 1975 Committee on Planetary and Lunar Exploration (Complex) Summer Study, Seattle, Washington, July 1975.

4. Vojvodich, N. S., et.al., "Outer Planet Atmospheric Entry Probes - An Overview of Technology Readiness," AIAA Paper No. 75-1147, September 1975.

5. Sutton, K., "Radiative Heating About Outer Planet Entry Probes," AIAA Paper No. 75-183, January 1975.

6. Nicolet, W. E., Mezines, S. A. and Balakrishnan, A., "Configuration Impact on Heat Shield Requirements for Jupiter Entry," AIAA Paper No. 76-470, to be presented at the 11th Thermophysics Conference, July 1976.

7. Kessler, W. C., "Test Evaluation of Potential Heat Shield Contamination of an Outer Planet Probe's Gas Sampling System," NASA CR-137619, January 1975.

8. Personal Communications with Don Schmidt and Rex Farmer of AFML.

9. Personal Communications with Stan Channon of Aerospace.

ACKNOWLEDGEMENTS

The writers are grateful to Mr. Donald Spinks for his persistent and diligent efforts in coordinating the heat shield fabrication activities and to Mr. James Smittkamp for his evaluation of the strength characteristics of the heat shield, fabrication approach and the mechanical property test data.